Semiannual Status Report

NASA-Ames Cooperative Agreement Number NCC 2-680

DIURNAL FORCING OF PLANETARY ATMOSPHERES

For the period July 1 through December 31, 1991

Submitted to

Dr. Robert M. Haberle, Technical Officer
National Aeronautics and Space Administration
Ames Research Center, MS 245-3
Moffett Field, California 94035

Prepared by

Dr. Howard C. Houben, Principal Investigator
Space Physics Research Institute
572 Hyannis Drive
Sunnyvale, California 94087-1315
(408) 736-9705

Progress Report

A free convection parameterization has been introduced into the Mars Planetary Boundary Layer Model (MPBL). Previously, the model would fail to generate turbulence under conditions of zero wind shear, even when statically unstable. This in turn resulted in erroneous results at the equator, for example, when the lack of Coriolis forcing allowed zero wind conditions. The underlying cause of these failures was the level 2 second-order turbulence closure scheme which derived diffusivities as algebraic functions of the Richardson number (the ratio of static stability to wind shear). In the previous formulation the diffusivities were scaled by the wind shear--a convenient parameter since it is non-negative. This has the drawback that all diffusivities are zero under conditions of zero shear (viz., the free convection case). The new scheme tests for the condition of zero shear in conjunction with static instability and recalculates the diffusivities using a static stability scaling. The results for a simulation of the equatorial boundary layer at autumnal equinox are presented in Figures 1-4. (Note that after some wind shear is generated, the model reverts to the traditional diffusivity calculation.)

As can be seen from Figures 1 and 3, the equatorial boundary layer simulation generates very strong winds (in the upslope direction) which appear to be accelerating even after the standard six day run. This is probably due to the total neglect of inertial terms (the Coriolis term is, of course, zero) in the equations of motion. Another possible culprit is the slope parameterization which attempts to integrate the hydrostatic law to determine surface pressure. It is recommended that the model move to a sigma (or hybrid) coordinate scheme wherein the atmospheric mass flux divergence is integrated to determine surface pressure variations.

The previously developed Nonlinear Balanced Model (NLBM) has been utilized to initialize the terrestrial version of the Mars Climate Model (which is optimized for stratospheric calculations) with National Meteorological Center (NMC) data for simulations of the El Chichon volcanic cloud. It is clear from Figures 5 and 6 that there are problems with the data in the tropics. Unfortunately this is the region of interest for the early evolution of the cloud. The NLBM removes the erroneous discontinuity in the data at the equator and obtains a plausible analyzed wind field (Figure 7). There is, however, only a very weak QBO in this analyzed field. Thus the westward advection of the main cloud is somewhat underestimated. Figure 8 depicts the transport of the cloud for an eighty day period. It is recommended that similar calculations be conducted for this year's Pinatubo cloud for which the quality of the data is far better.

Resolution tests are being conducted with the Mars Climate Model (MCM) to determine the optimum configuration for running the model in annual water vapor transport simulations. Figures 9-14 demonstrate some of the results. In general, the mean fields are fairly well represented in the simulation with maximum wavenumber 10. The eddies are well represented in a simulation with maximum wavenumber 20. Tests involving lower resolution in the vertical and zonal directions will be conducted in the future.

Future Work

As mentioned above, resolution tests of the MCM will be continued. Of importance is the issue of whether the resolution required by the model is a function of dust optical depth. There is also a need to explore the performance of (and necessity for) the high altitude sponge layer as the model's upper boundary is moved down and resolution is reduced.

Given the good performance of the terrestrial version of the MCM in transporting the El Chichon volcanic cloud, the model will be applied to extensive studies of the mid-winter transport of Martian water vapor under both clear and dusty conditions.

It is expected that two papers describing (1) the MPBL and the simulation of Viking Lander meteorology and (2) the MPBL and its coupled subsurface model of the water vapor diurnal cycle will be published in the near future.

Figure Captions

Figure 1. MPBL results for a simulation at the equator at the autumnal equinox (Ls = 180). Other parameters of the simulation are: thermal inertia = 360 SI; visible optical depth = 0.30; infrared optical depth = 0.15; albedo = 0.25; surface pressure = 6.1 mb. The surface winds are always directed in the upslope direction as there is no Coriolis forcing to change the wind heading from the forcing direction.

Figure 2. Planetary boundary layer height as a function of time for the simulation described in Figure 1. The equatorial boundary layer appears to reach very great heights.

Figure 3. Wind magnitude near the ground for the simulation in Figure 1. (Again all winds are in the upslope direction.) The lack of any inertial terms apparently allows the wind to grow to very high magnitudes. The only dissipative effect is surface friction. The slope parameterization (and perhaps the penetration height for the ground's thermal effect--7 km in this run) must be re-examined for this simulation.

Figure 4. The potential temperature as a function of altitude and time for the simulation of Figure 1. The thermal components of the MPBL appear to be functioning quite well in this simulation.

Figure 5. The geopotential height of the 50 mb surface as a function of latitude and longitude as reported by the National Meterological Center for April 5, 1982 (the approximate time of the main El Chichon eruption). Note the apparent discontinuity near the equator which must be an artifact of the data analysis process.

Figure 6. The mean zonal wind in gradient wind balance with the NMC geopotentials of Figure 5. Note the noise in the data at low latitudes near the 30 mb level, the region of primary interest for the early transport of the El Chichon aerosols.

Figure 7. The mean zonal wind analyzed by the NLBM for the geopotentials of Figure 5. A step function at the equator is removed from the data to obtain a smooth wind field. However, the QBO is very weak in the analyzed field, probably too weak to give the observed rapid westward advection of the cloud.

Figure 8. Latitude-longitude plots of the predicted relative optical depth of the El Chichon cloud at 10 day intervals after the eruption. The general trends of strong easterly advection with approximate confinement of the main cloud between the equator and 30 degrees north latitude are consistent with the observations. Contour levels are spaced logarithmic with each level being greater than the previous one by a factor of the square root of 10.

Figure 9. A comparison of the zonal mean temperatures (20 day averages after 80 days of computation) for mid-winter simulations of the clear Martian atmosphere with maximum wavenumbers of (a) 20 and (b) 10. (The standard MCM simulations have been conducted with maximum wavenumber 30.) There is little to choose between these temperature fields except for the low altitude inversion present in most of the domain of 9b. This is probably caused by an inability to fully resolve the condensation flow of carbon dioxide to the north (winter) pole.

Figure 10. As in Figure 9, but for the vertical velocity. The vertical velocity, being driven primarily by diabatic processes is similar in the two simulations.

Figure 11. As in Figure 9, but for the mean zonal wind. Note the very strong surface winds in the low maximum wavenumber case. This is apparently due to inadequate wave activity in the low resolution case.

Figure 12. As in Figure 9, but for the temperature eddy amplitude in the bottom layer of the model. In the low resolution case, most baroclinic eddy activity is concentrated in zonal wavenumber 1. The higher resolution case much more closely resembles the standard case.

Figure 13. As in Figure 12, but for the meridional wind eddy amplitude. Again the low resolution case wave activity is concentrated in wavenumber 1 and apparently spans all latitudes.

Figure 14. As in Figure 9, but for the residual circulation, a measure of the advective component of both the mean circulation and the eddies. At low altitudes near 60 degrees north latitude, there are significant differences between the two model runs (again due to the different eddy characteristics). This is the region of interest for the Martian water vapor cycle.

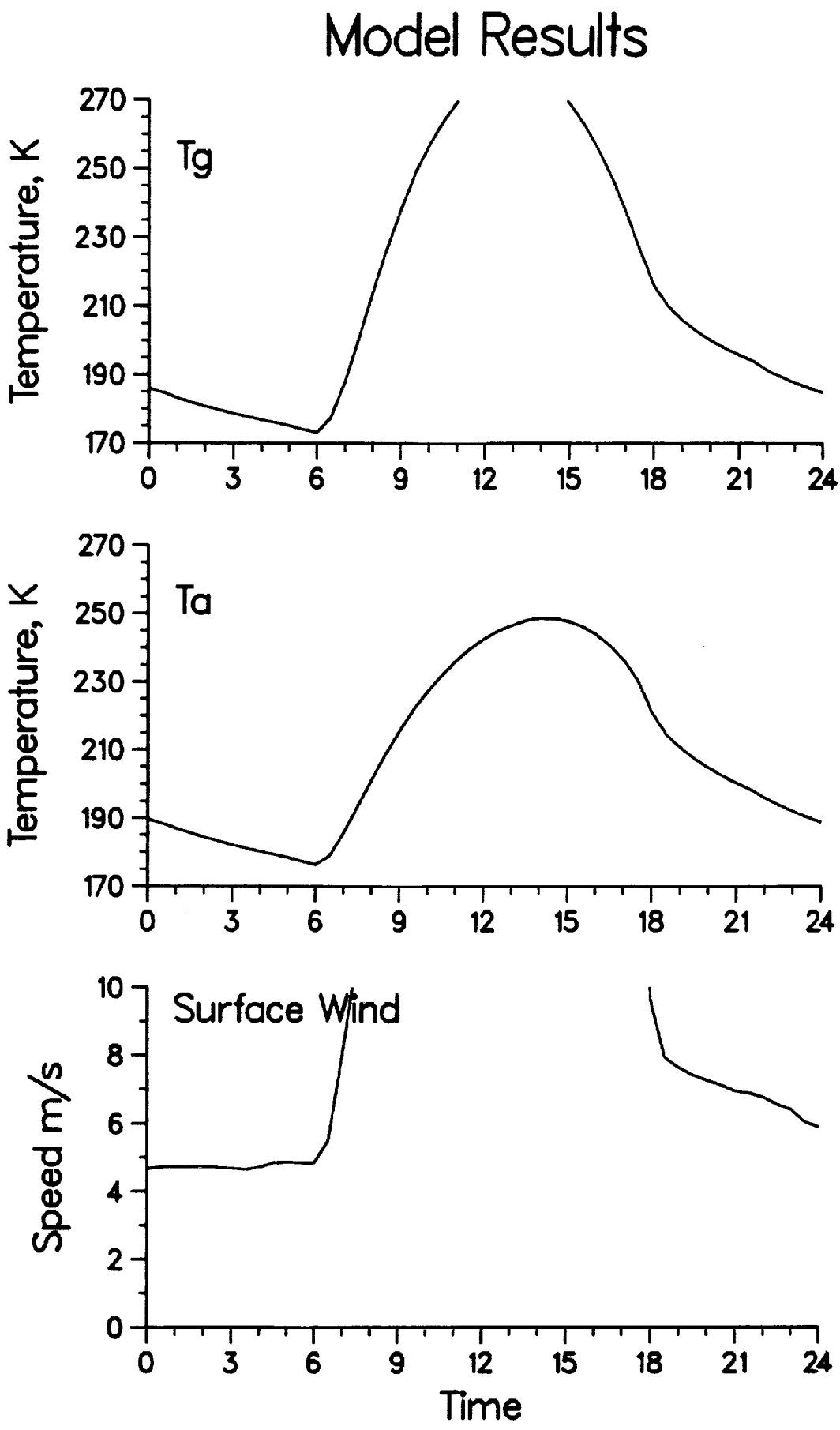
Model Results
Tg
Temperature, K
270
250
230
210
190
170
0
3
6
9
12
15
18
21
24
Ta
Temperature, K
Surface Wind
Speed m/s
10
8
6
4
2
0
Time

Figure 1.

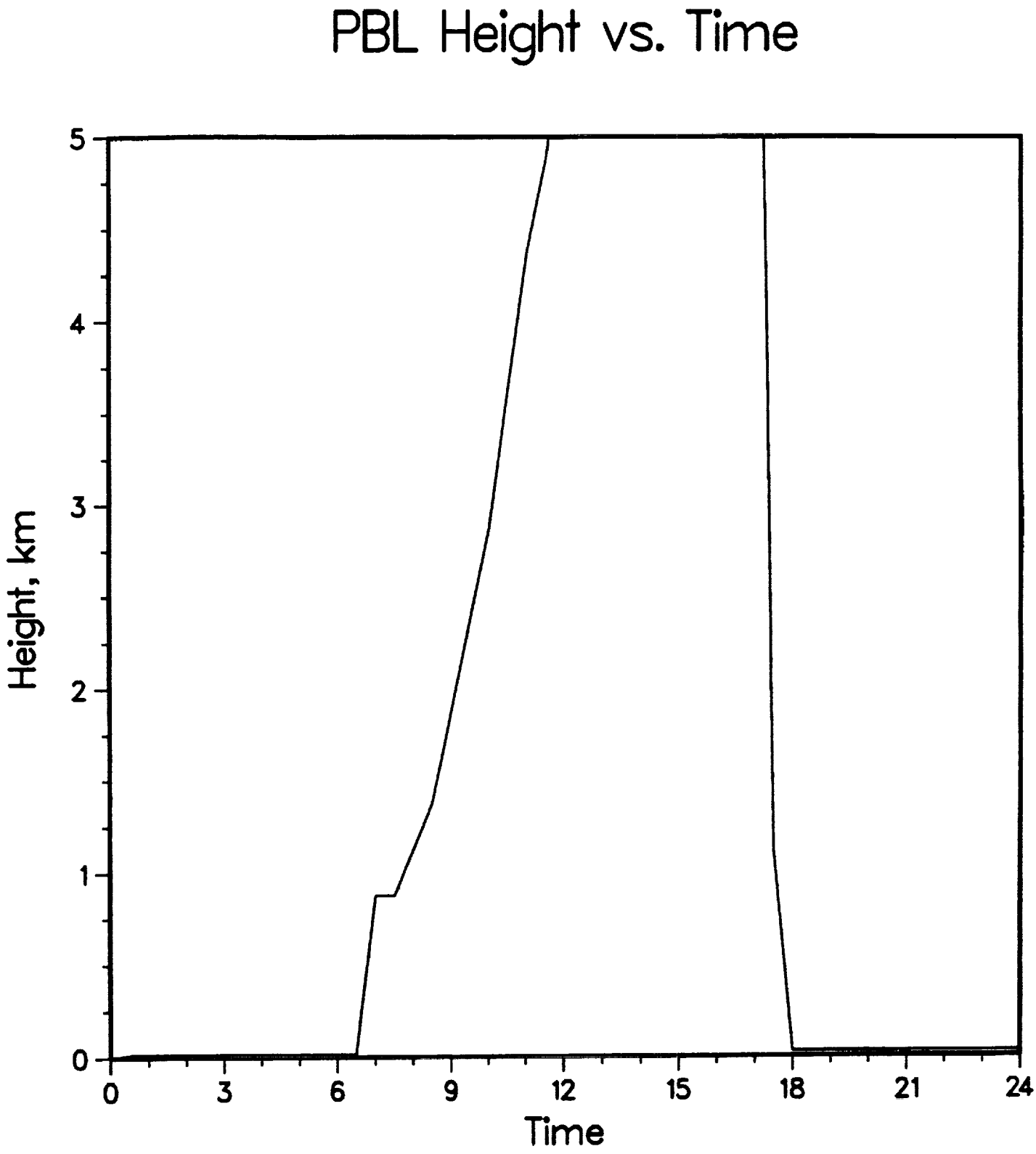

Figure 2.

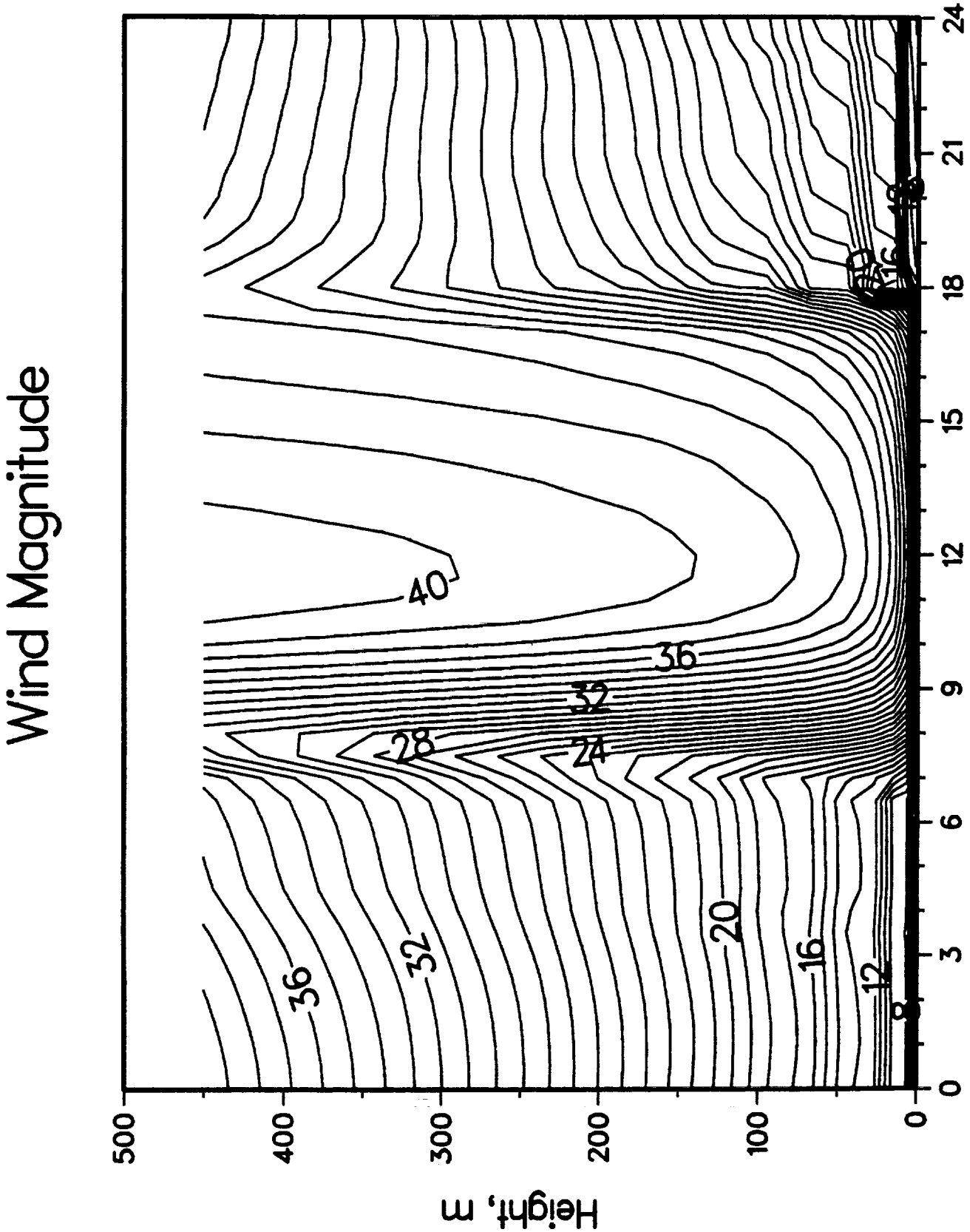
Wind Magnitude
Height, m
Time, hr
500
400
300
200
100
0
0
3
6
9
12
15
18
21
24
40
36
32
28
24
20
16
12
8

Figure 3.

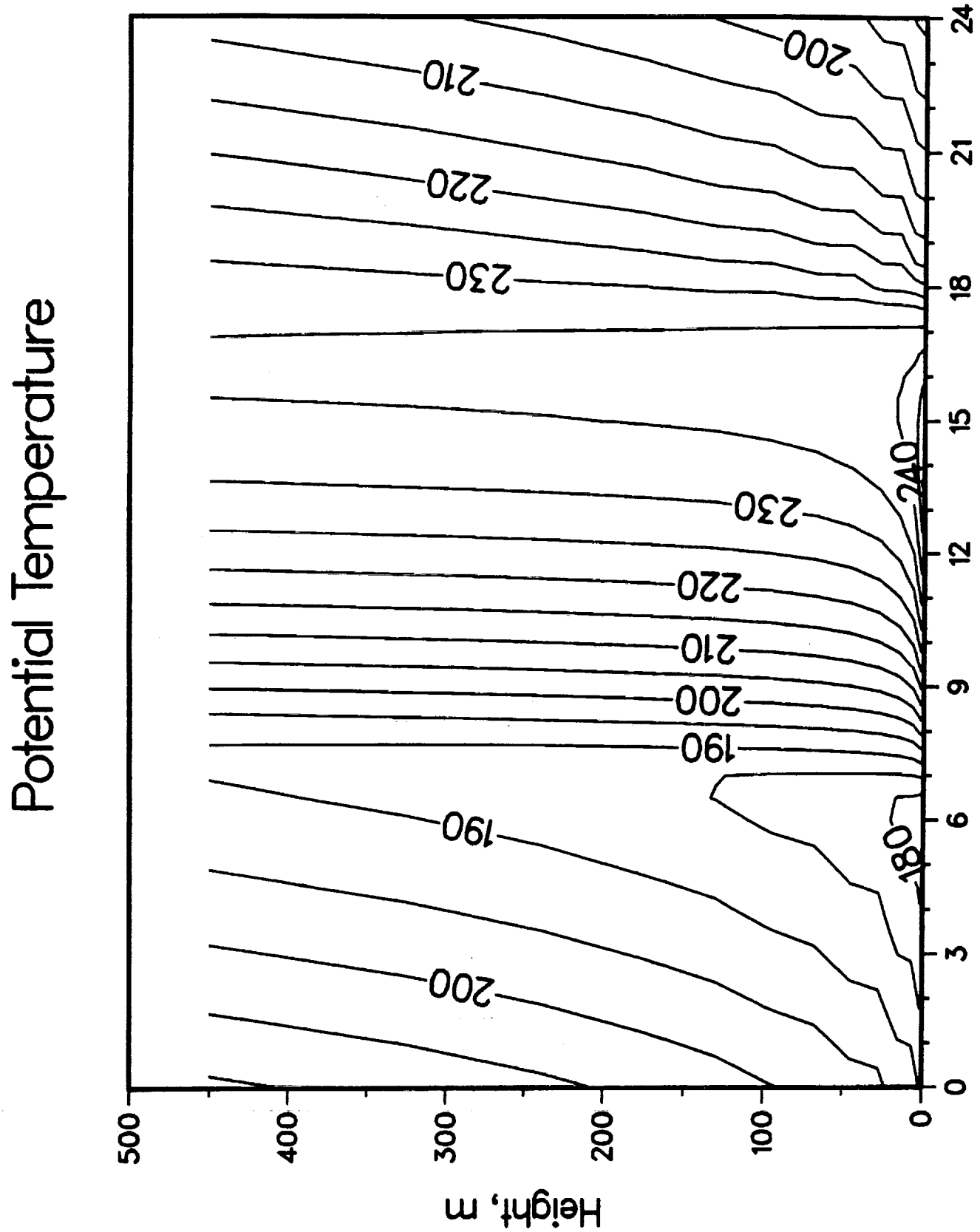
Potential Temperature
Height, m
Time, hr
0
100
200
300
400
500
0
3
6
9
12
15
18
21
24
180
190
200
210
220
230
240

Figure 4.

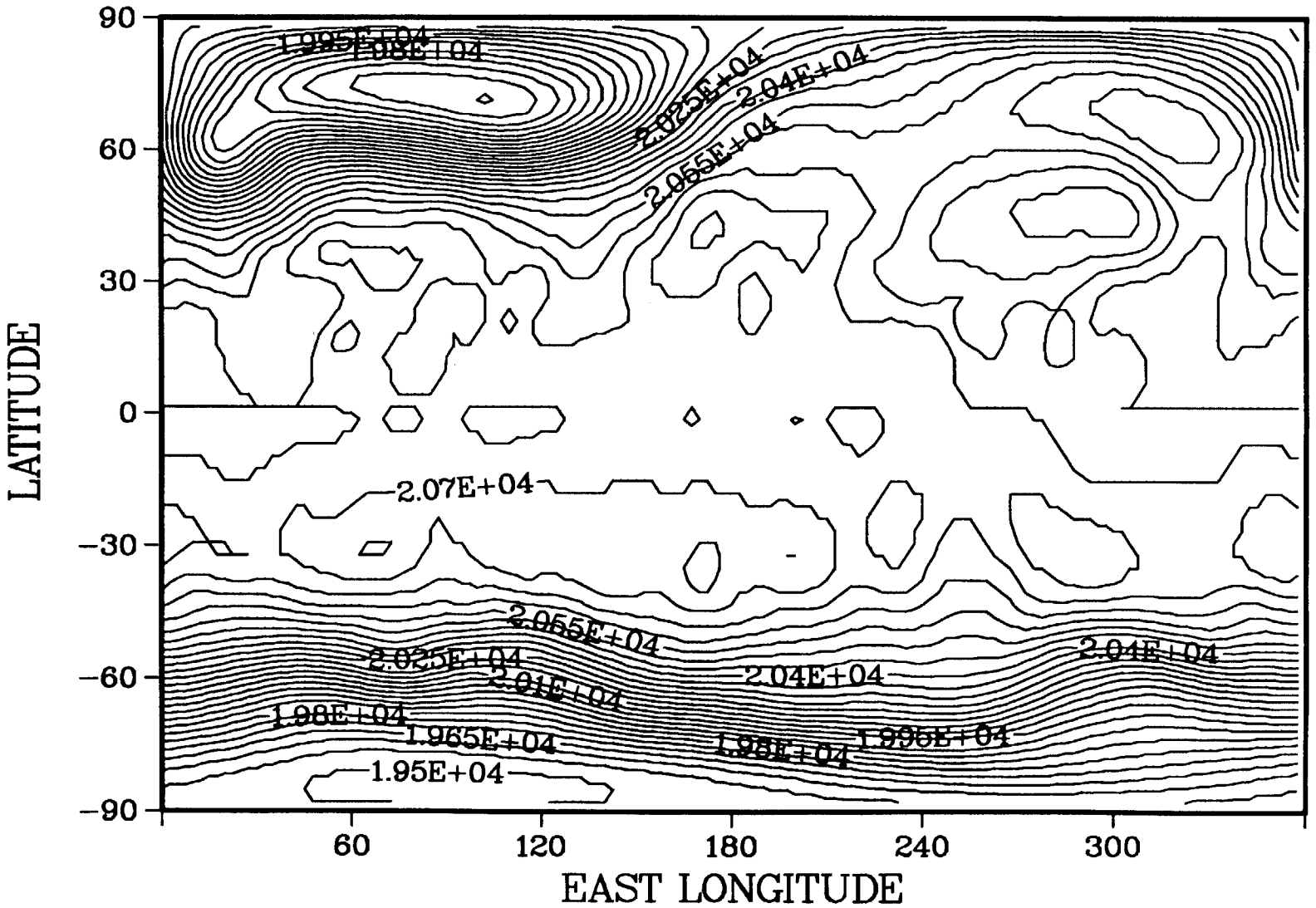
GEOPOTENTIAL HEIGHT 50mbar
90
60
30
0
-30
-60
-90
LATITUDE
60
120
180
240
300
EAST LONGITUDE
1.995E+04
1.98E+04
2.025E+04
2.04E+04
2.055E+04
2.07E+04
2.055E+04
2.025E+04
2.01E+04
2.04E+04
2.04E+04
1.98E+04
1.965E+04
1.98E+04
1.995E+04
1.95E+04

Figure 5.

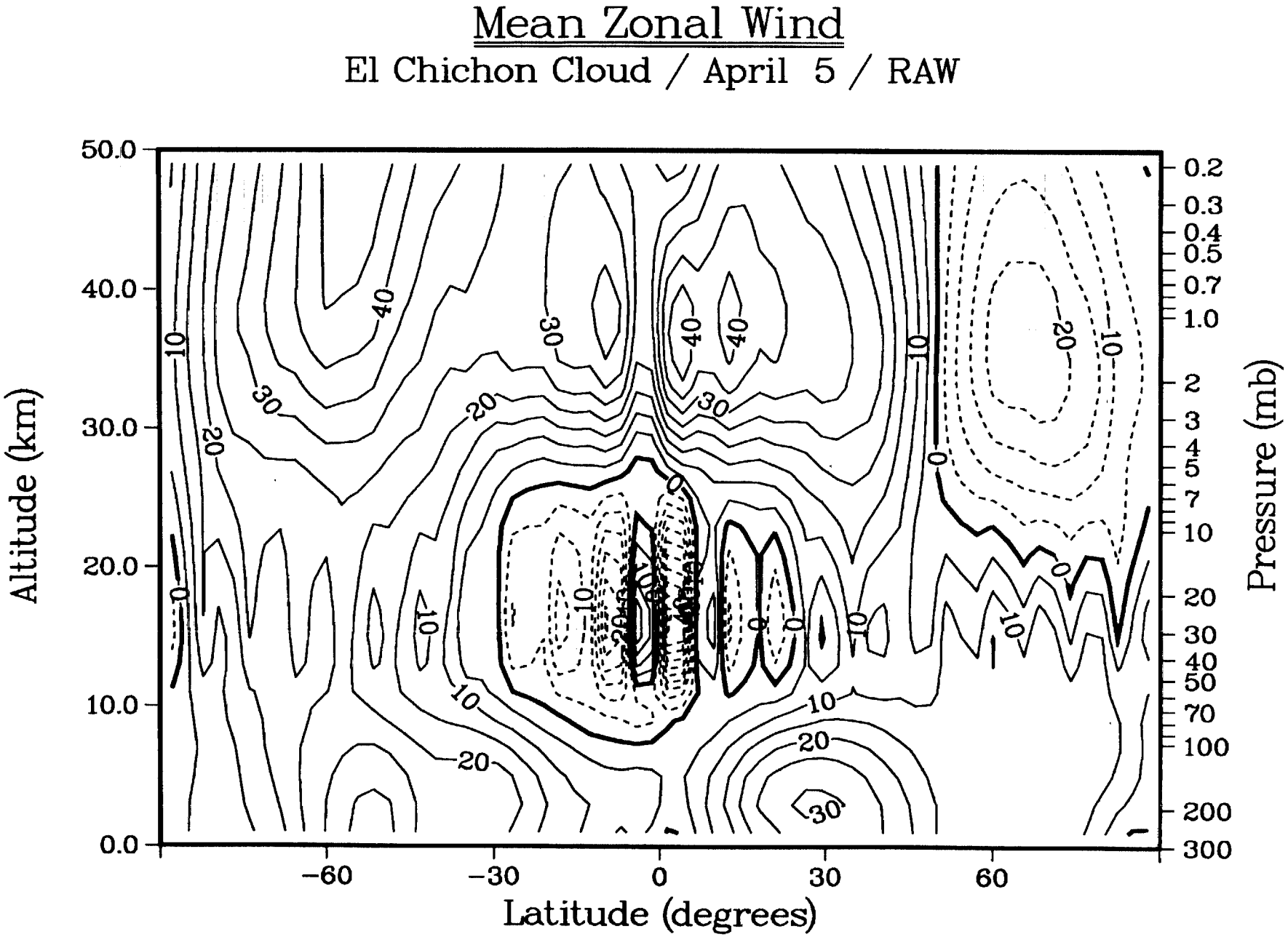
Mean Zonal Wind
El Chichon Cloud / April 5 / RAW
Altitude (km)
50.0
40.0
30.0
20.0
10.0
0.0
Pressure (mb)
0.2
0.3
0.4
0.5
0.7
1.0
2
3
4
5
7
10
20
30
40
50
70
100
200
300
−60
−30
0
30
60
Latitude (degrees)

Figure 6.

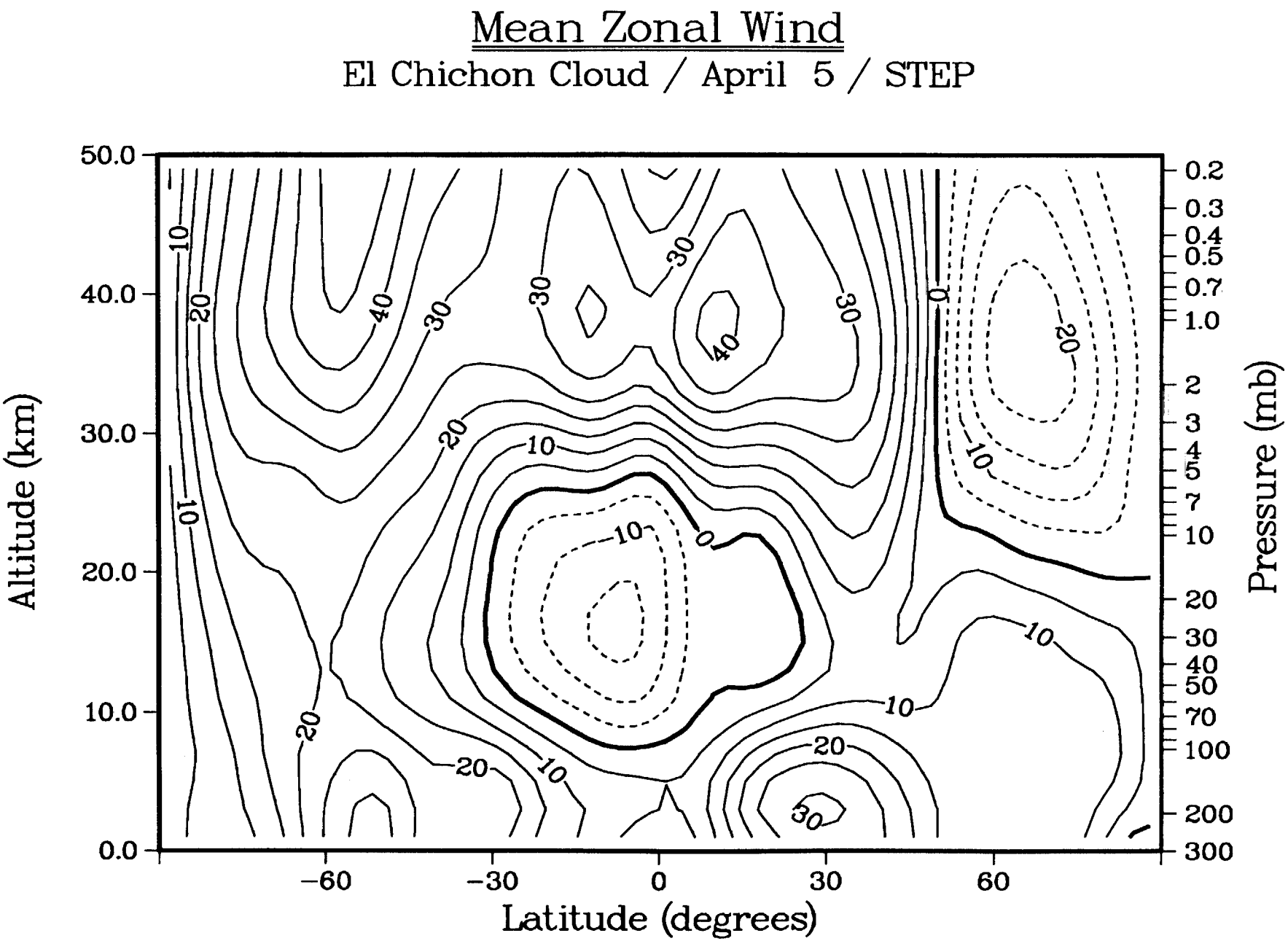
Mean Zonal Wind
El Chichon Cloud / April 5 / STEP
Altitude (km)
50.0
40.0
30.0
20.0
10.0
0.0
Pressure (mb)
0.2
0.3
0.4
0.5
0.7
1.0
2
3
4
5
7
10
20
30
40
50
70
100
200
300
−60
−30
0
30
60
Latitude (degrees)

Figure 7.

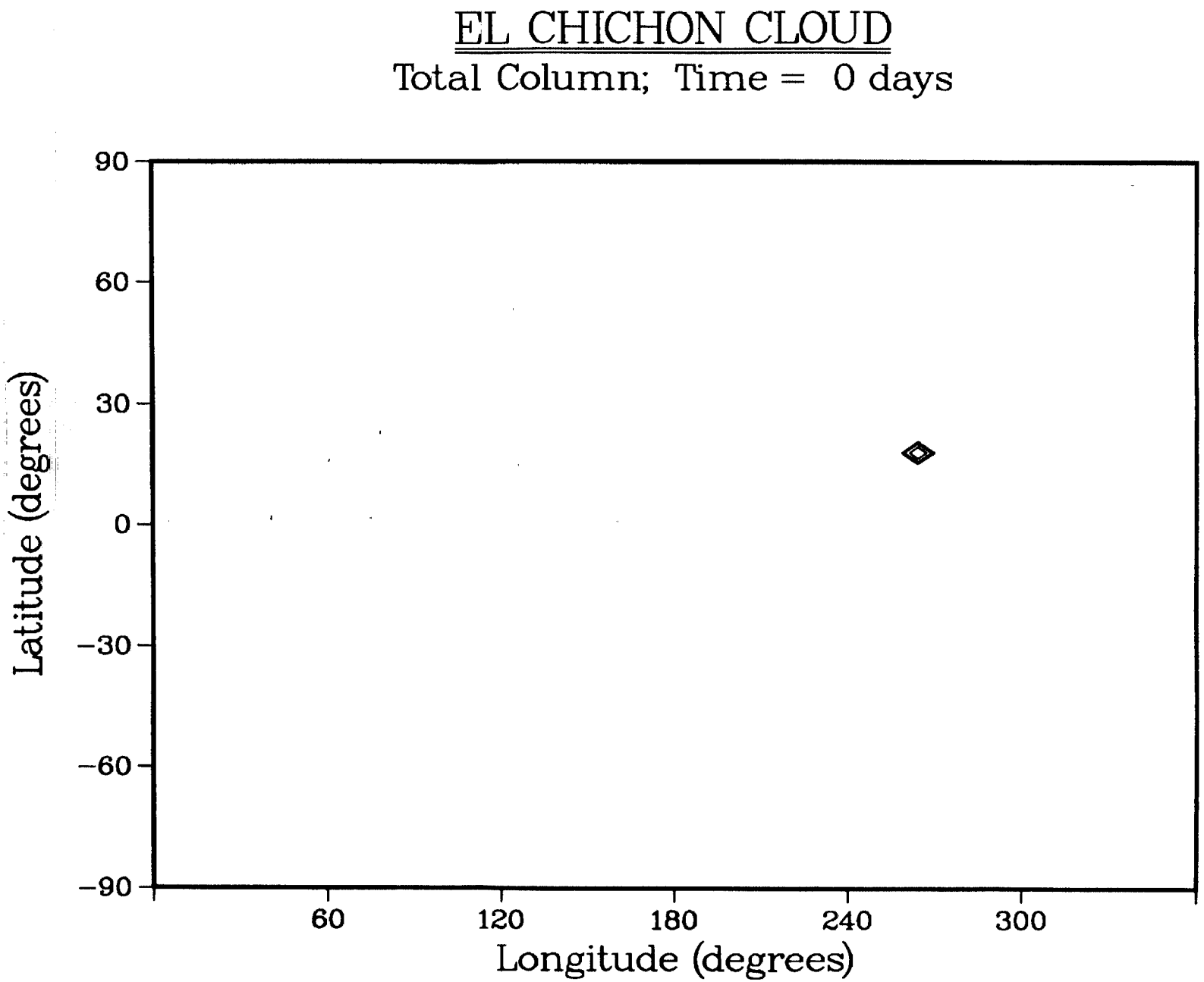
EL CHICHON CLOUD
Total Column; Time = 0 days
90
60
30
0
-30
-60
-90
Latitude (degrees)
60
120
180
240
300
Longitude (degrees)

Figure 8a.

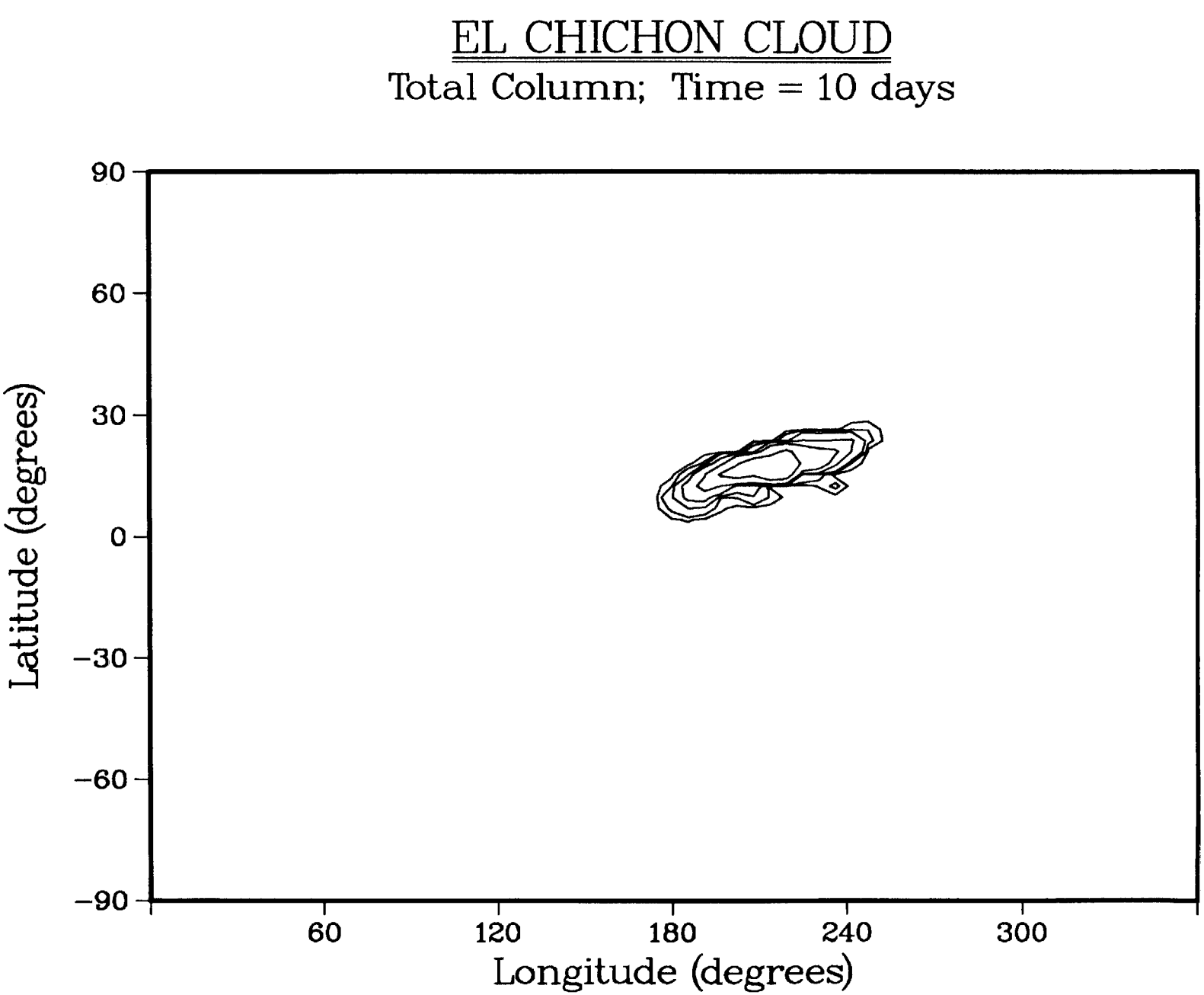
EL CHICHON CLOUD
Total Column; Time = 10 days
90
60
30
0
-30
-60
-90
Latitude (degrees)
60
120
180
240
300
Longitude (degrees)

Figure 8b.

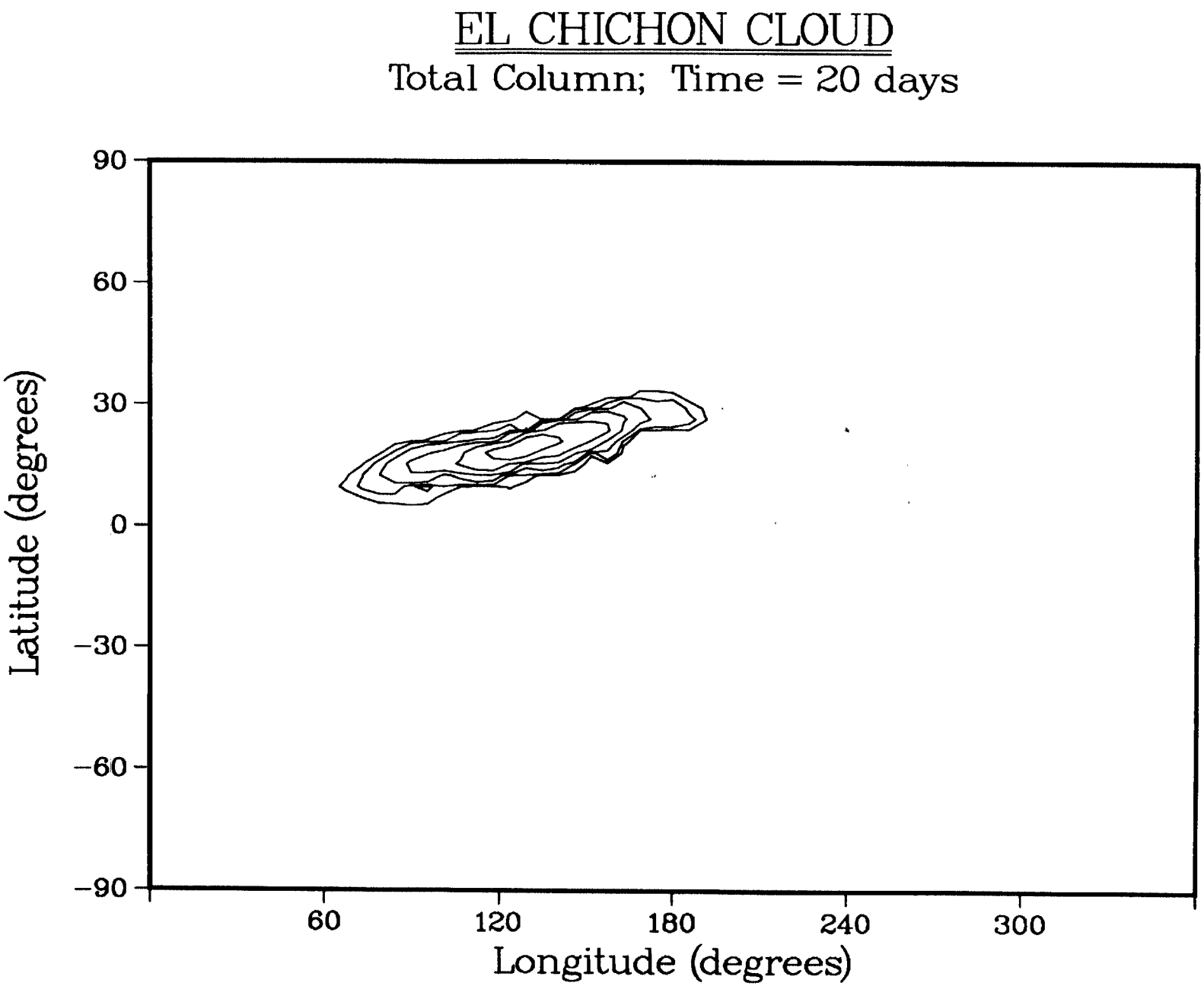
EL CHICHON CLOUD
Total Column; Time = 20 days
90
60
30
0
-30
-60
-90
Latitude (degrees)
60
120
180
240
300
Longitude (degrees)

Figure 8c.

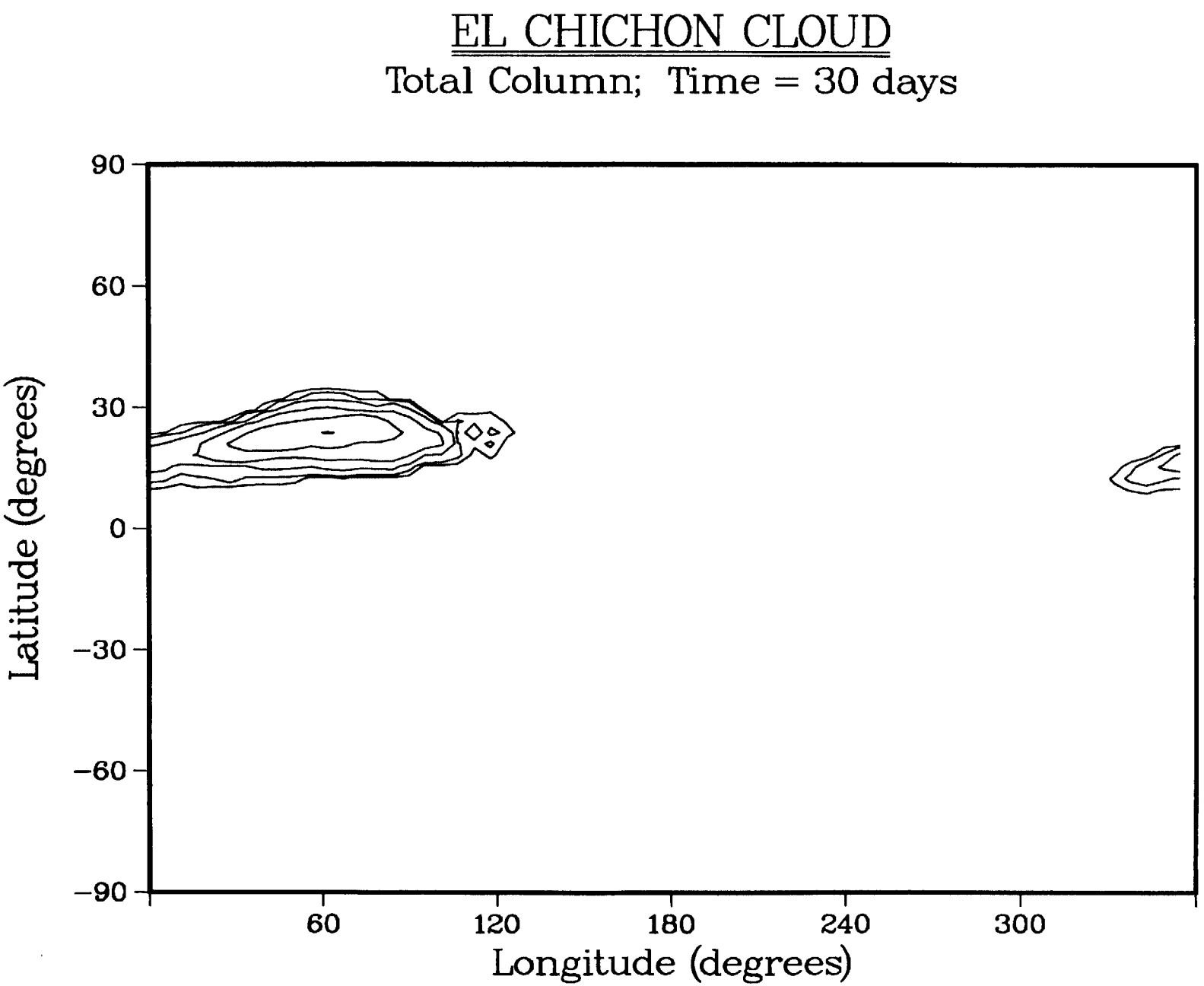
EL CHICHON CLOUD
Total Column; Time = 30 days
90
60
30
0
−30
−60
−90
Latitude (degrees)
60
120
180
240
300
Longitude (degrees)

Figure 8d.

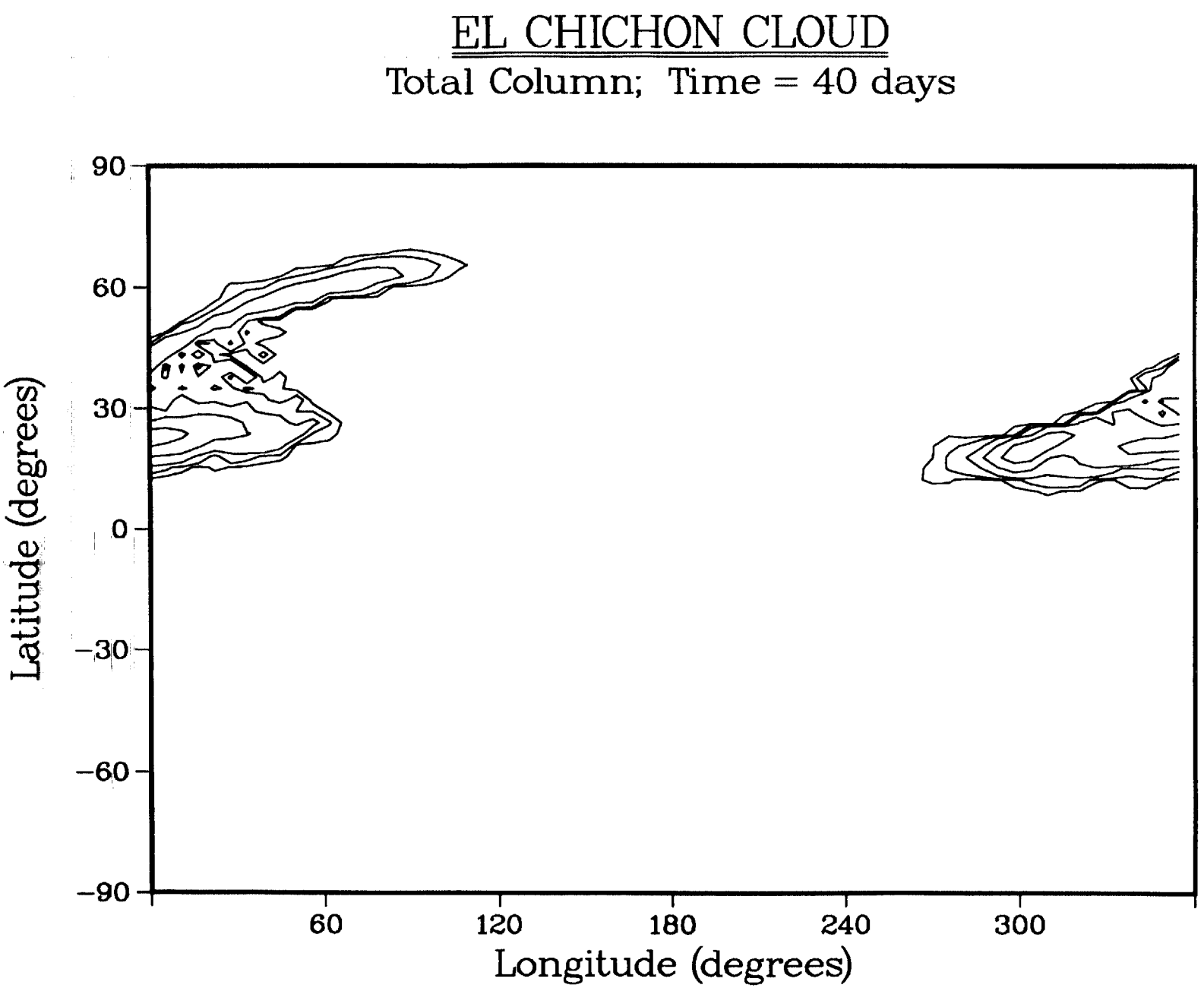
EL CHICHON CLOUD
Total Column; Time = 40 days
90
60
30
0
-30
-60
-90
Latitude (degrees)
60
120
180
240
300
Longitude (degrees)

Figure 8e.

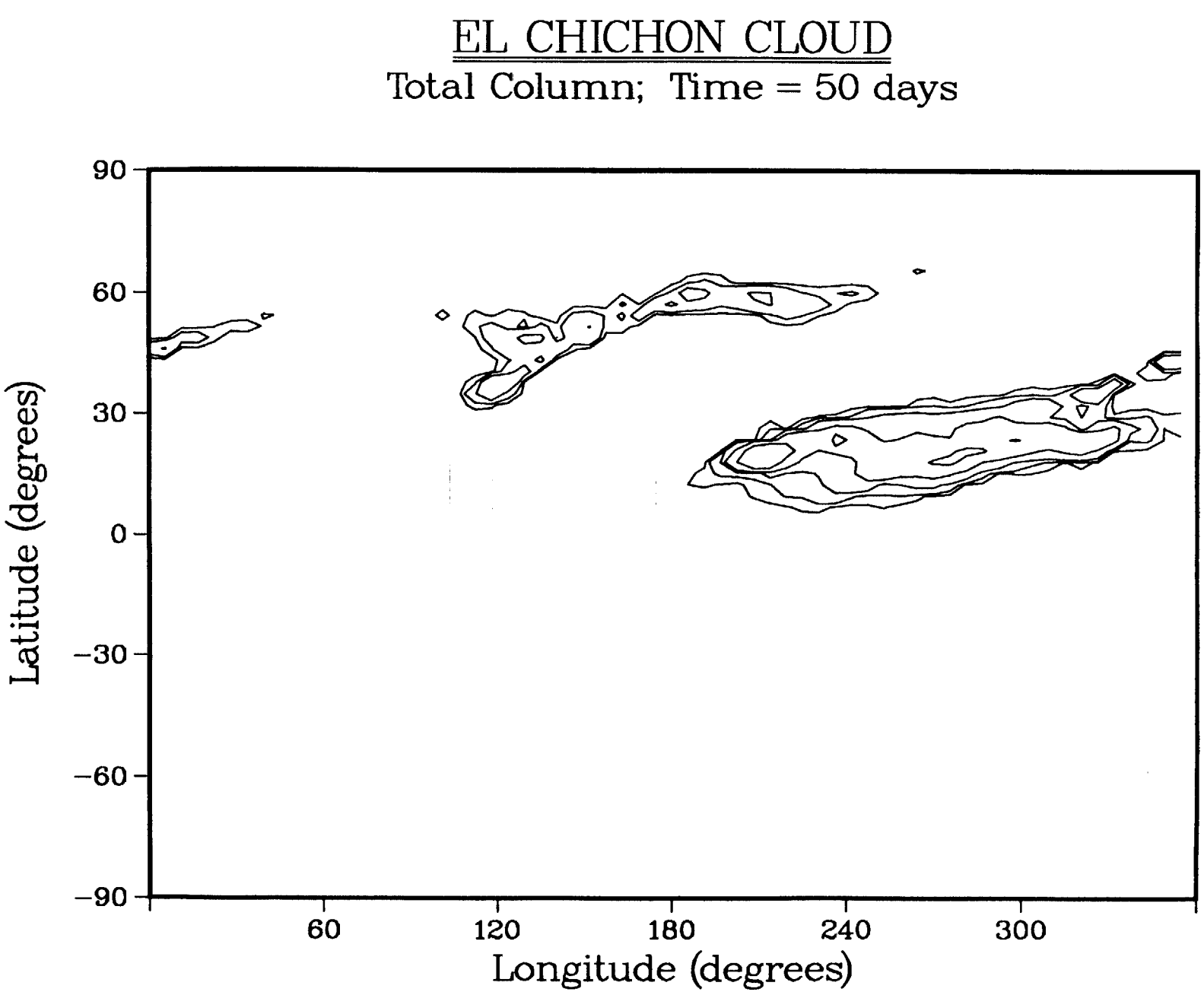
EL CHICHON CLOUD
Total Column; Time = 50 days
90
60
30
0
-30
-60
-90
Latitude (degrees)
60
120
180
240
300
Longitude (degrees)

Figure 8f.

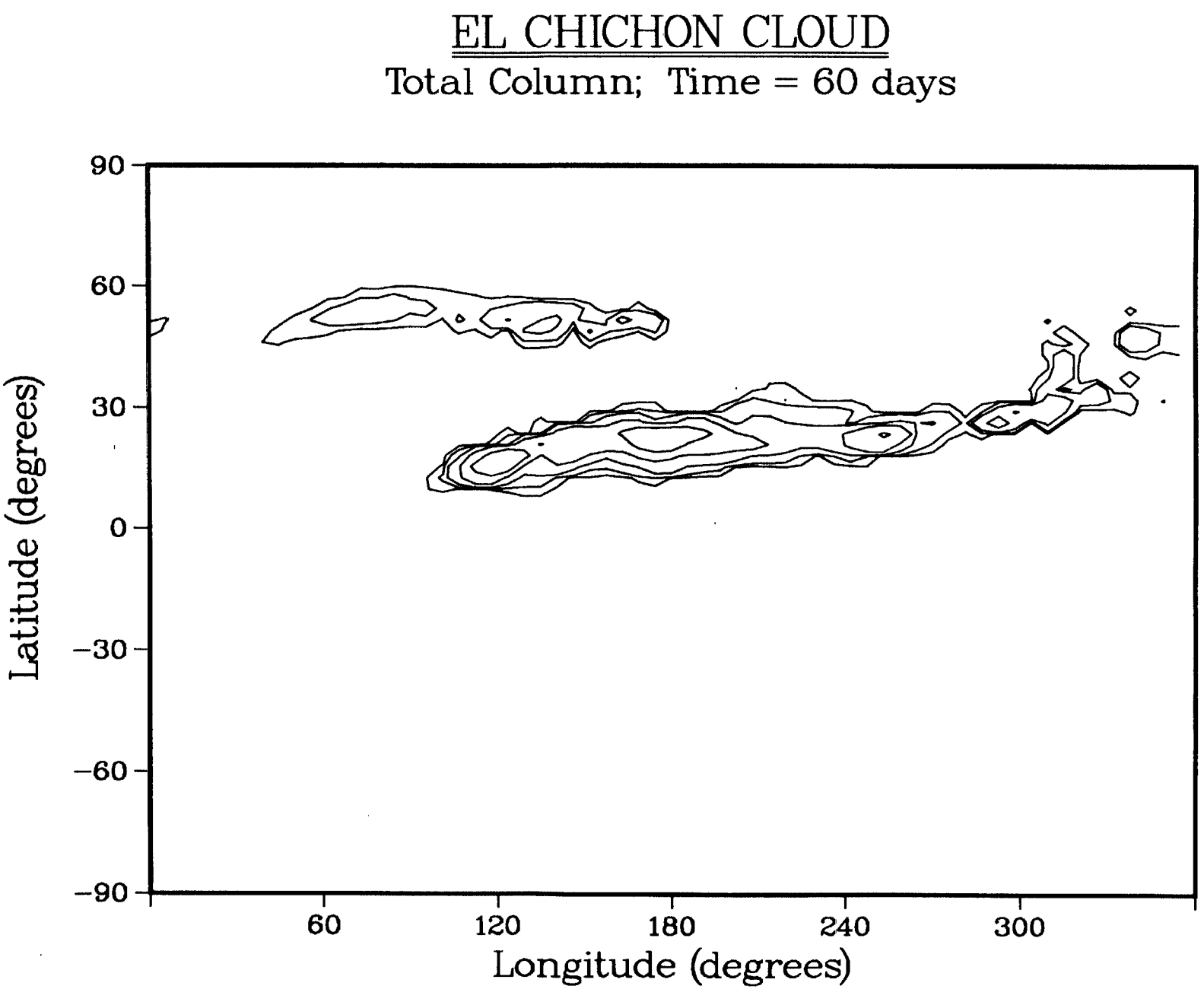
EL CHICHON CLOUD
Total Column; Time = 60 days
90
60
30
0
-30
-60
-90
Latitude (degrees)
60
120
180
240
300
Longitude (degrees)

Figure 8g.

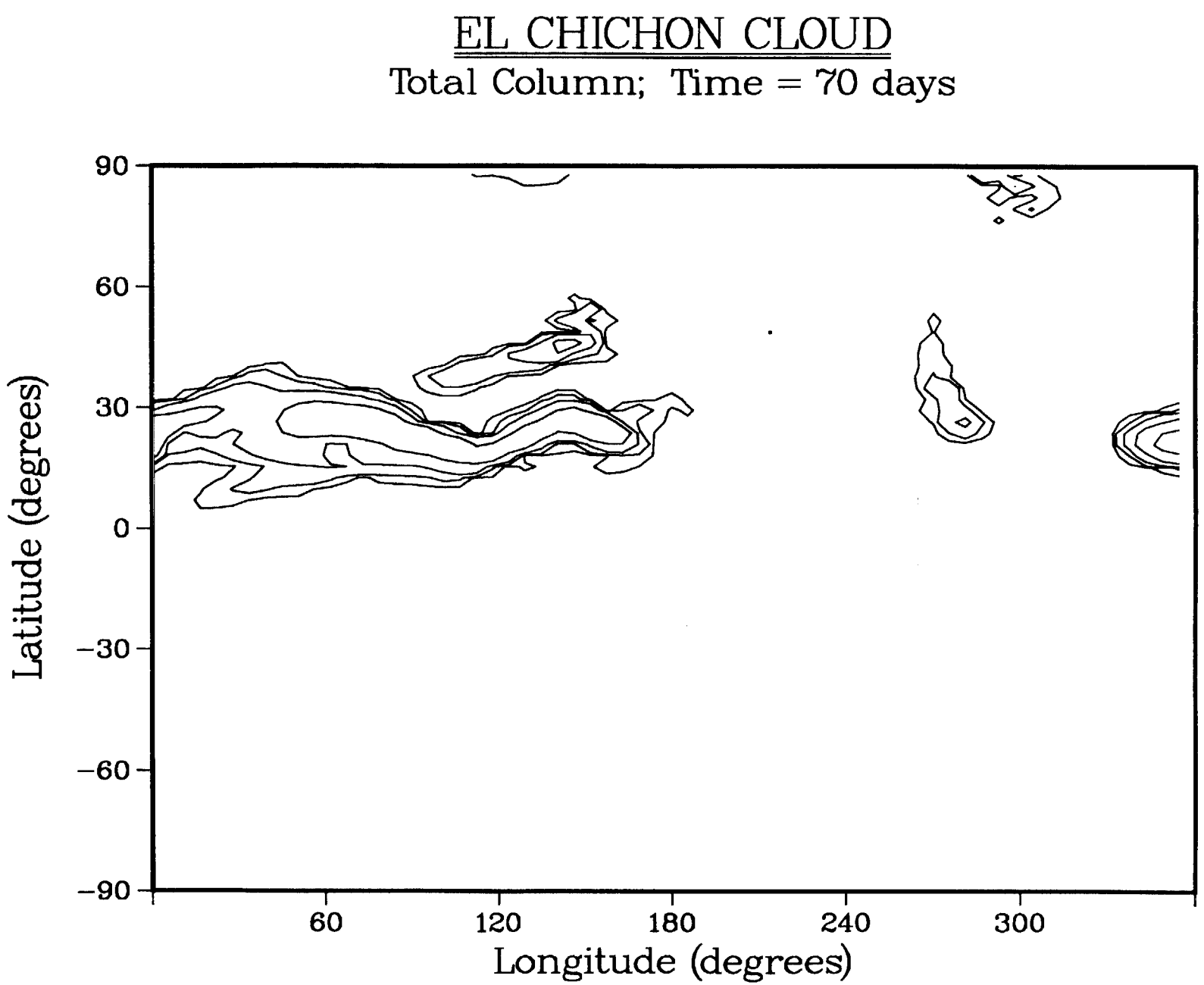
EL CHICHON CLOUD
Total Column; Time = 70 days
90
60
30
0
-30
-60
-90
Latitude (degrees)
60
120
180
240
300
Longitude (degrees)

Figure 8h.

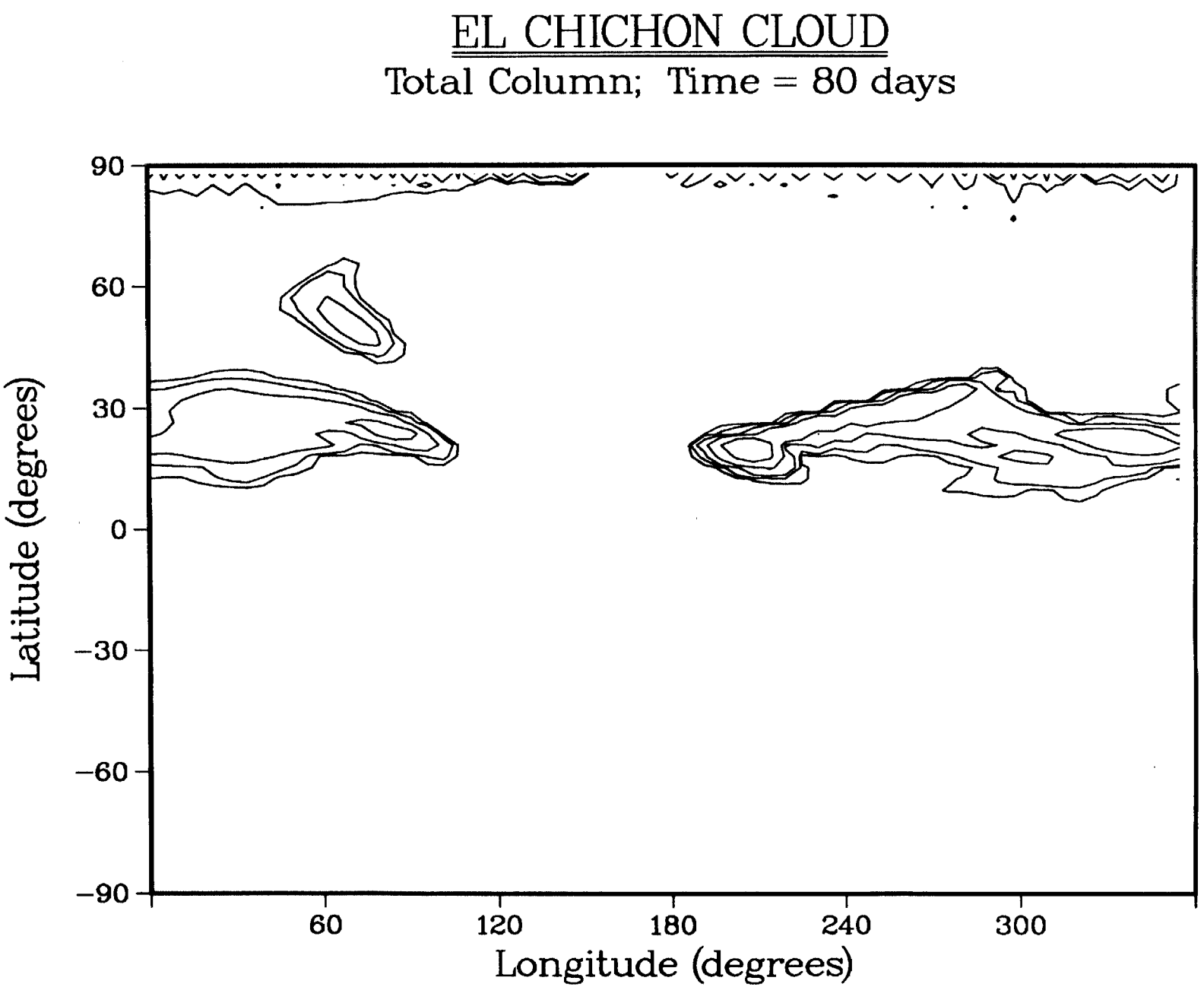
EL CHICHON CLOUD
Total Column; Time = 80 days
90
60
30
0
-30
-60
-90
Latitude (degrees)
60
120
180
240
300
Longitude (degrees)

Figure 8i.

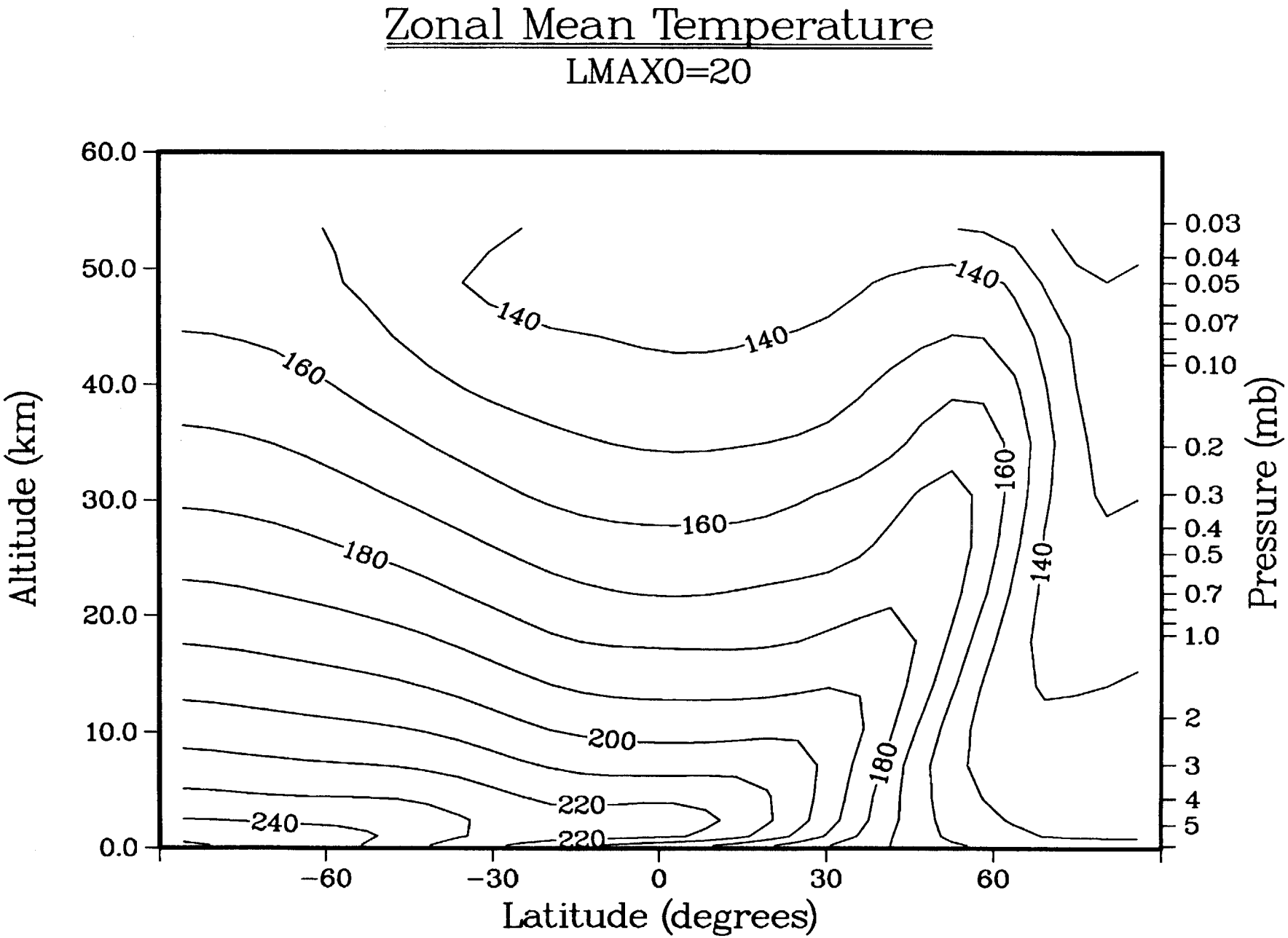
Zonal Mean Temperature
LMAX0=20
Altitude (km)
60.0
50.0
40.0
30.0
20.0
10.0
0.0
Pressure (mb)
0.03
0.04
0.05
0.07
0.10
0.2
0.3
0.4
0.5
0.7
1.0
2
3
4
5
140
140
140
160
160
160
180
180
200
220
220
240
-60
-30
0
30
60
Latitude (degrees)

Figure 9a.

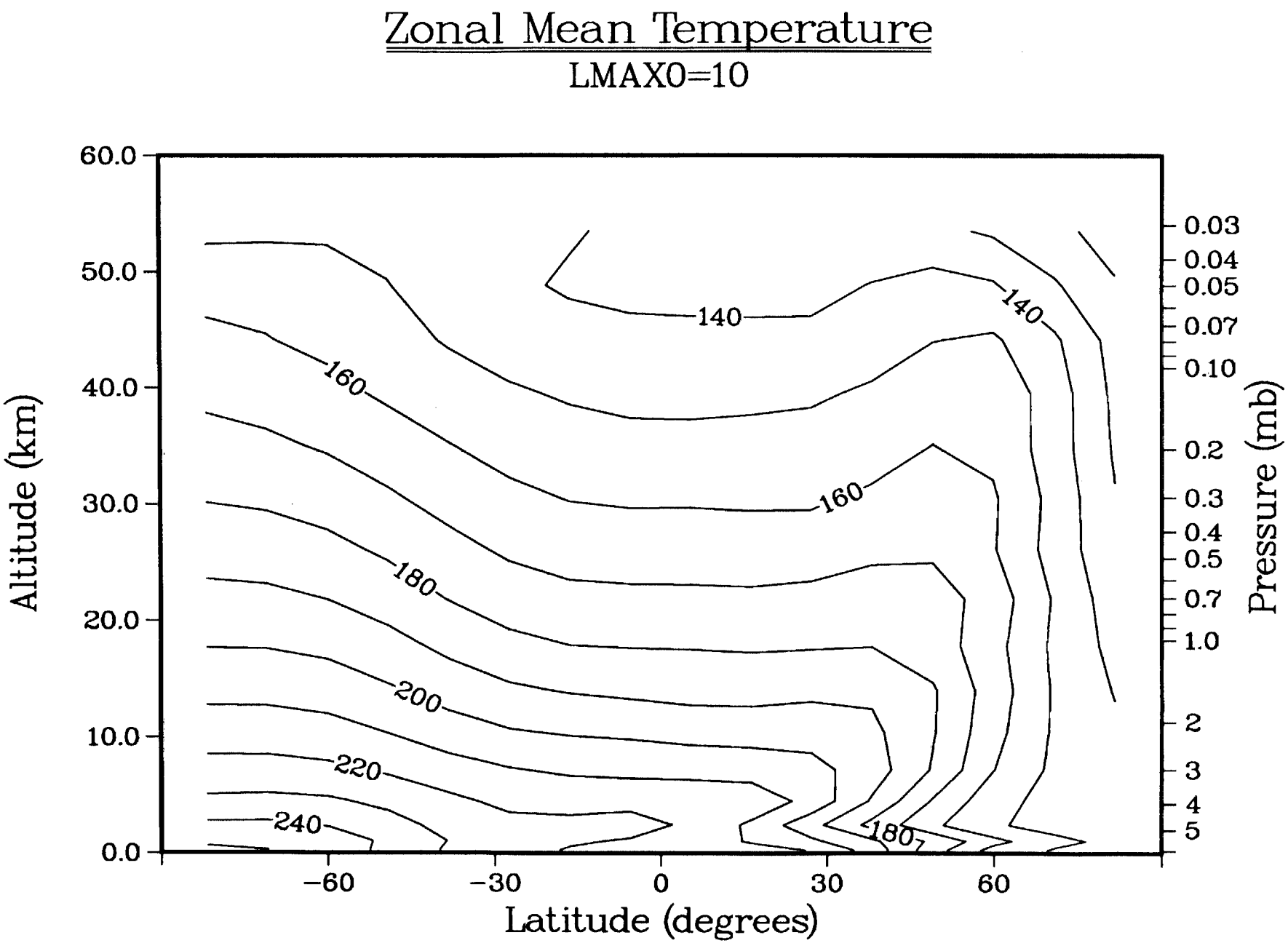
Zonal Mean Temperature
LMAX0=10
Altitude (km)
60.0
50.0
40.0
30.0
20.0
10.0
0.0
Pressure (mb)
0.03
0.04
0.05
0.07
0.10
0.2
0.3
0.4
0.5
0.7
1.0
2
3
4
5
140
140
160
160
180
180
200
220
240
−60
−30
0
30
60
Latitude (degrees)

Figure 9b.

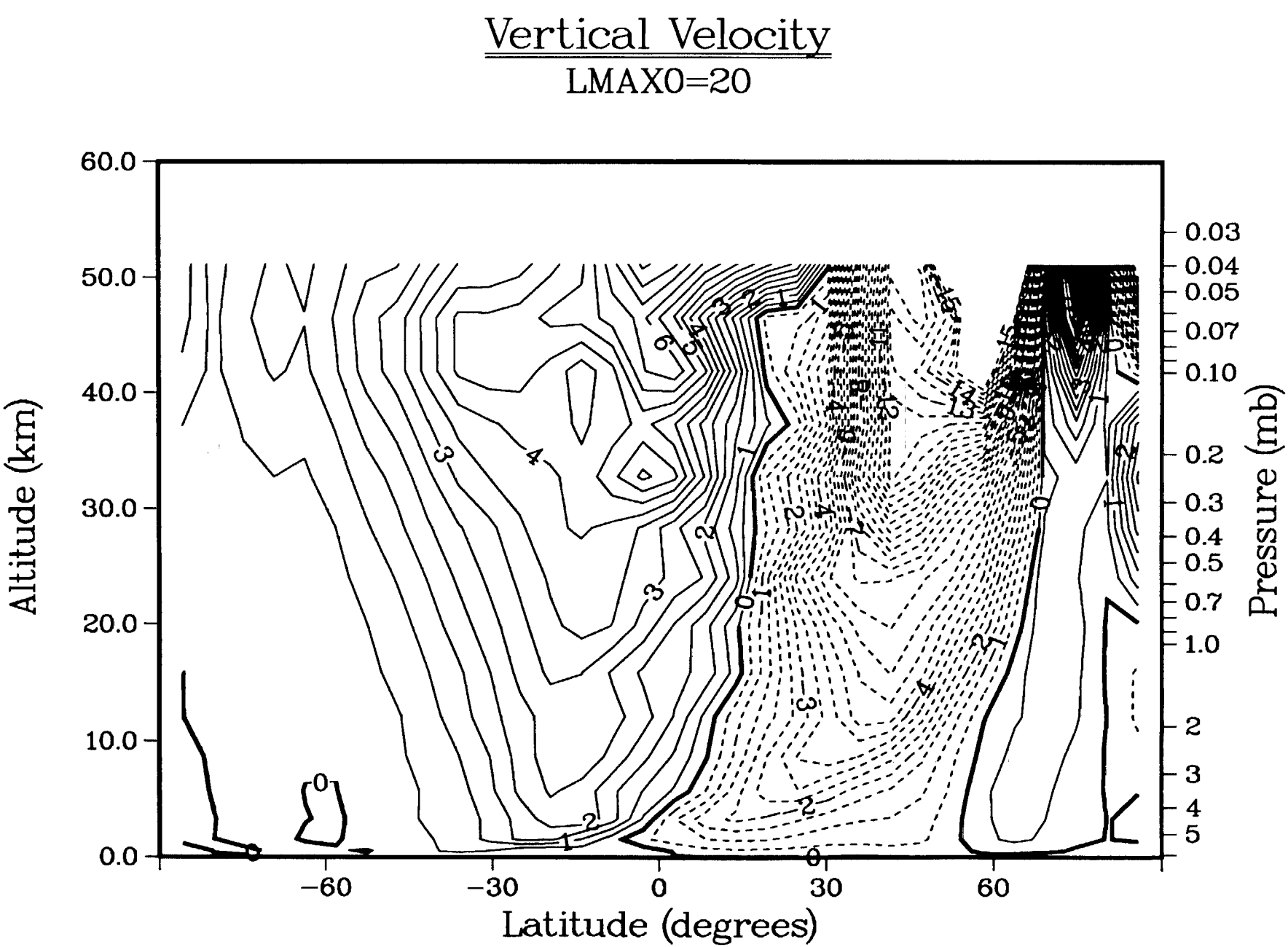
Vertical Velocity
LMAX0=20
Altitude (km)
60.0
50.0
40.0
30.0
20.0
10.0
0.0
Pressure (mb)
0.03
0.04
0.05
0.07
0.10
0.2
0.3
0.4
0.5
0.7
1.0
2
3
4
5
−60
−30
0
30
60
Latitude (degrees)

Figure 10a.

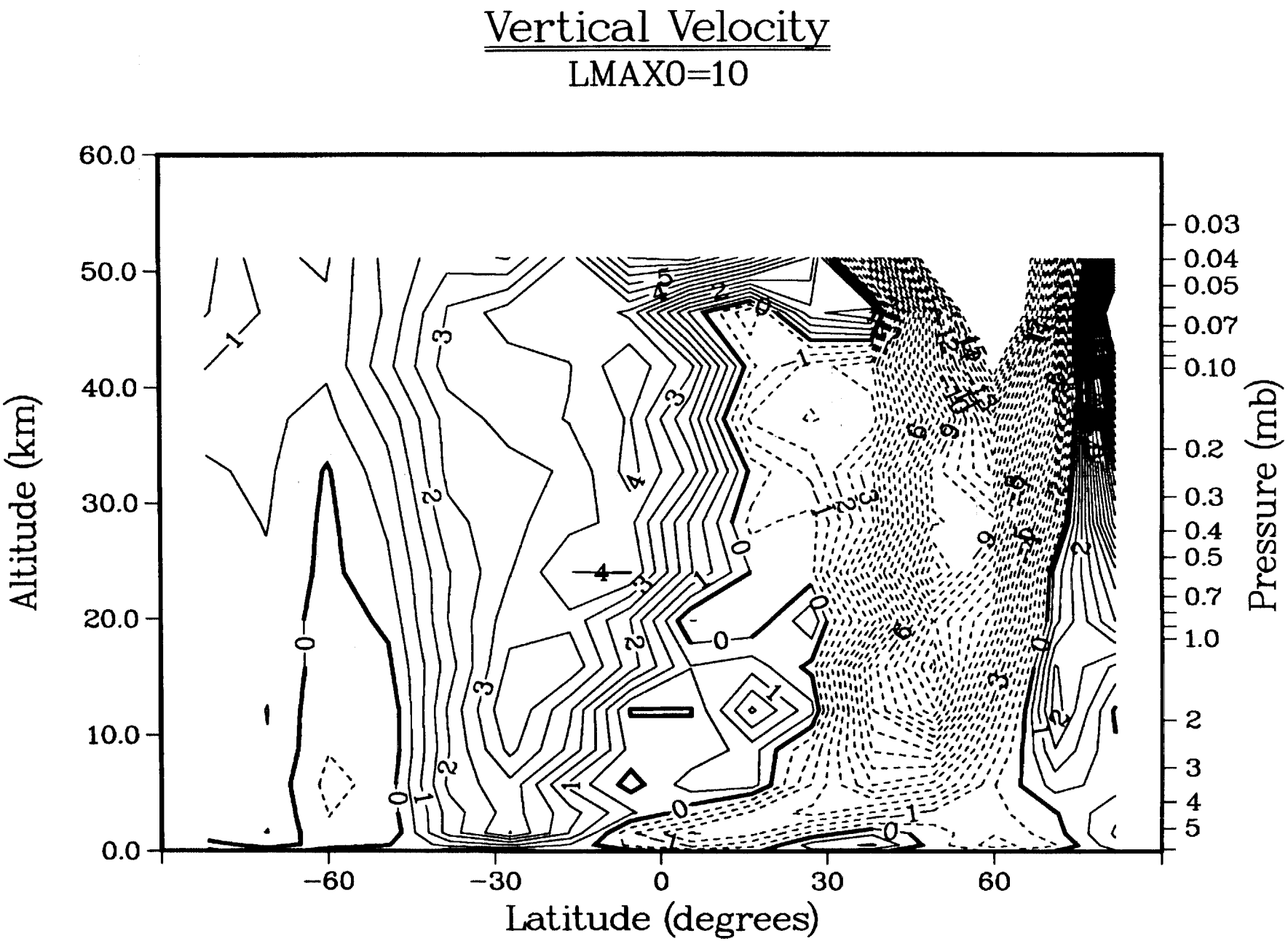
Vertical Velocity
LMAX0=10
Altitude (km)
60.0
50.0
40.0
30.0
20.0
10.0
0.0
Pressure (mb)
0.03
0.04
0.05
0.07
0.10
0.2
0.3
0.4
0.5
0.7
1.0
2
3
4
5
−60
−30
0
30
60
Latitude (degrees)

Figure 10b.

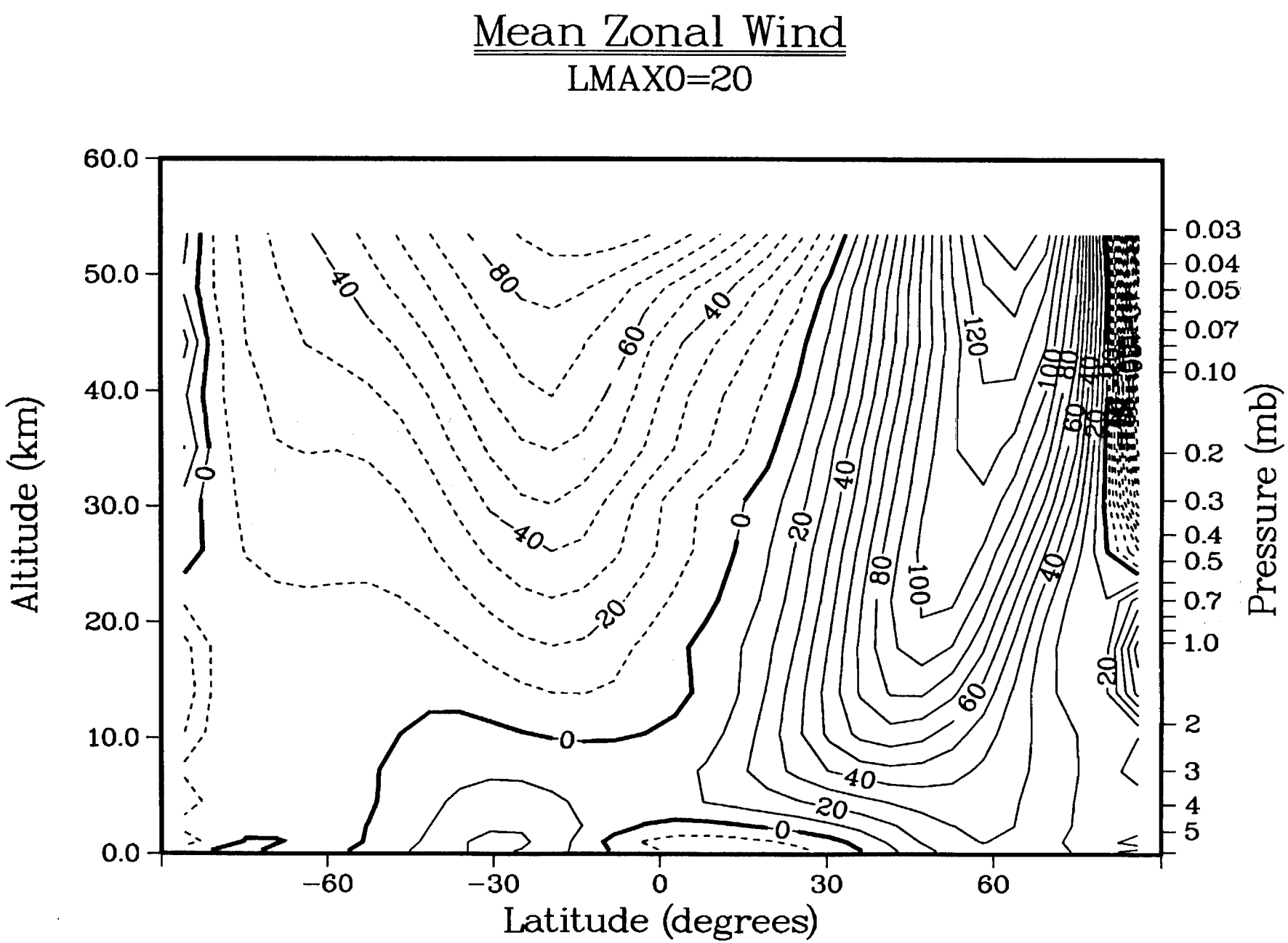
Mean Zonal Wind
LMAX0=20
Altitude (km)
60.0
50.0
40.0
30.0
20.0
10.0
0.0
Pressure (mb)
0.03
0.04
0.05
0.07
0.10
0.2
0.3
0.4
0.5
0.7
1.0
2
3
4
5
-60
-30
0
30
60
Latitude (degrees)

Figure 11a.

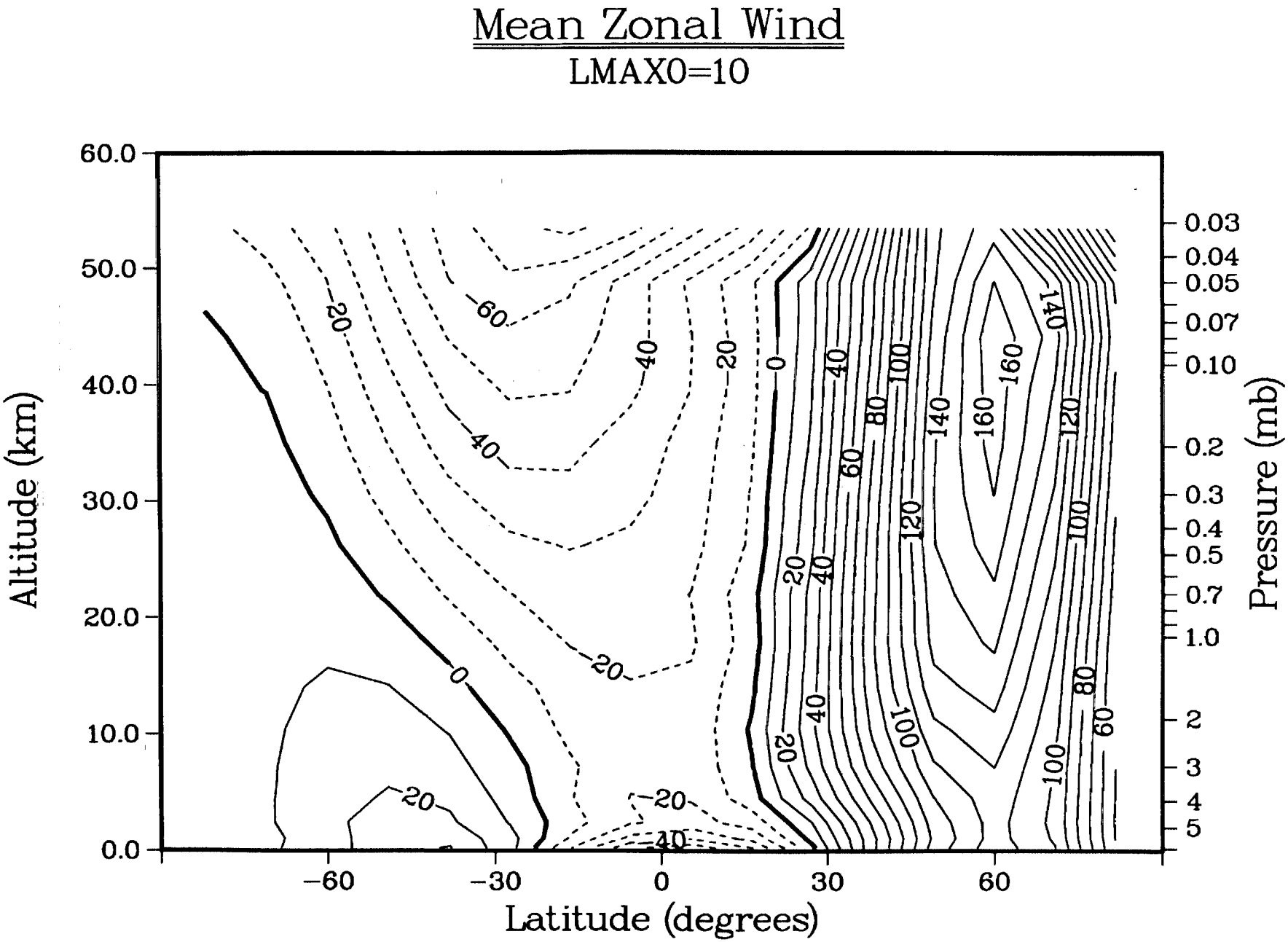
Mean Zonal Wind
LMAX0=10
Altitude (km)
Pressure (mb)
Latitude (degrees)
60.0
50.0
40.0
30.0
20.0
10.0
0.0
0.03
0.04
0.05
0.07
0.10
0.2
0.3
0.4
0.5
0.7
1.0
2
3
4
5
-60
-30
0
30
60

Figure 11b.

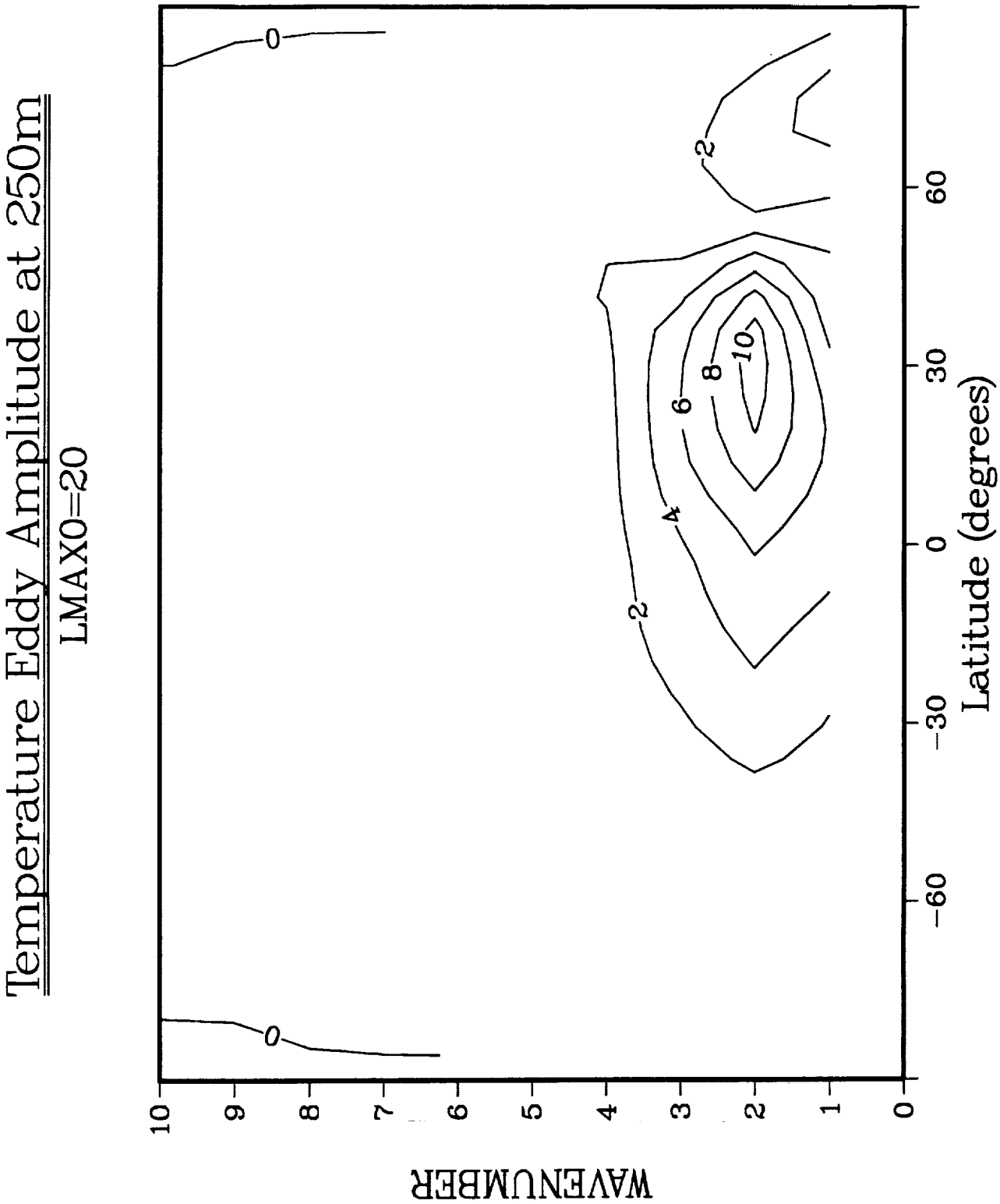
Temperature Eddy Amplitude at 250m
LMAX0=20
WAVENUMBER
Latitude (degrees)
0
1
2
3
4
5
6
7
8
9
10
-60
-30
0
30
60
0
0
2
2
4
6
8
10

Figure 12a.

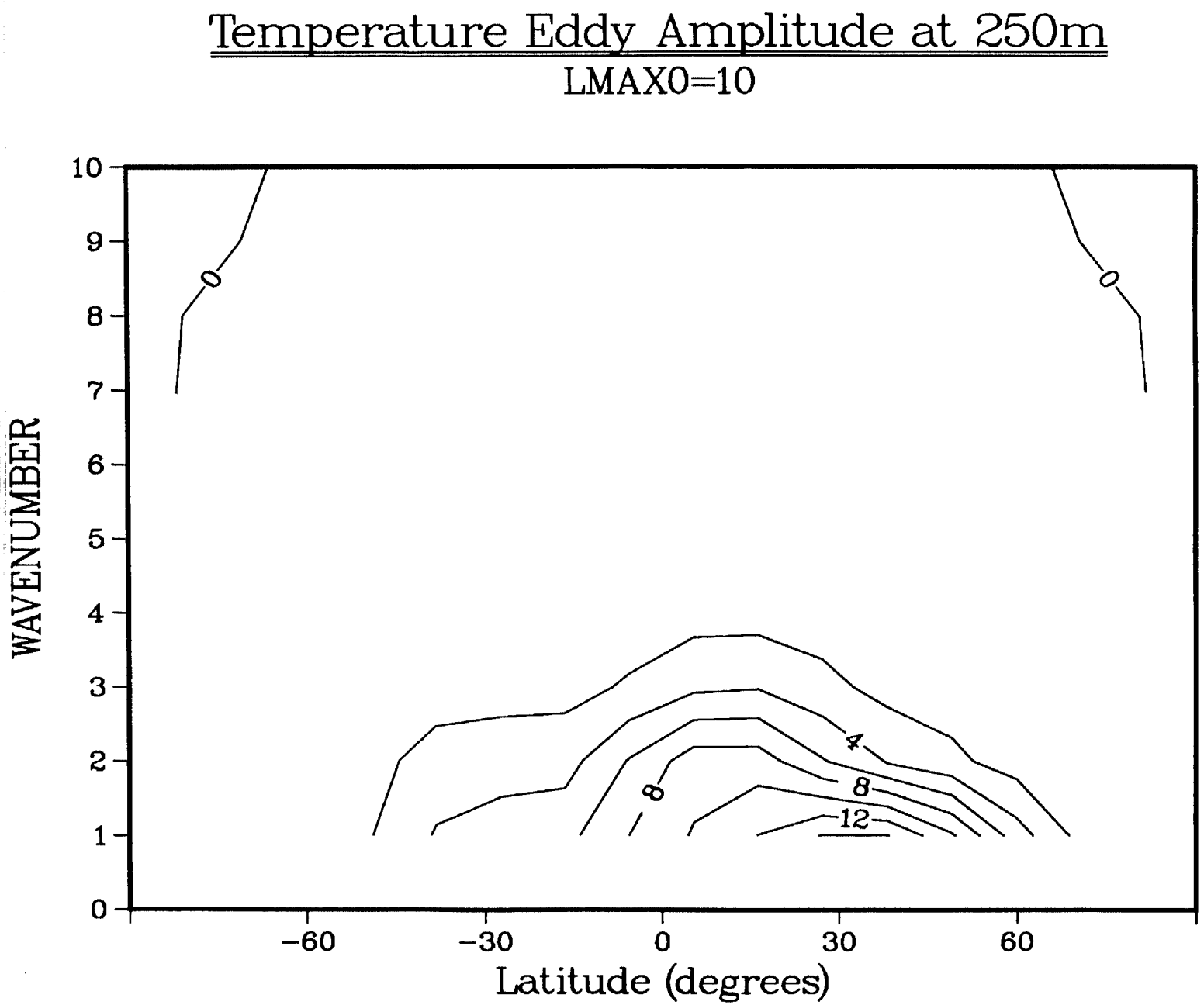
Temperature Eddy Amplitude at 250m
LMAX0=10
WAVENUMBER
10
9
8
7
6
5
4
3
2
1
0
0
0
4
8
8
12
−60
−30
0
30
60
Latitude (degrees)

Figure 12b.

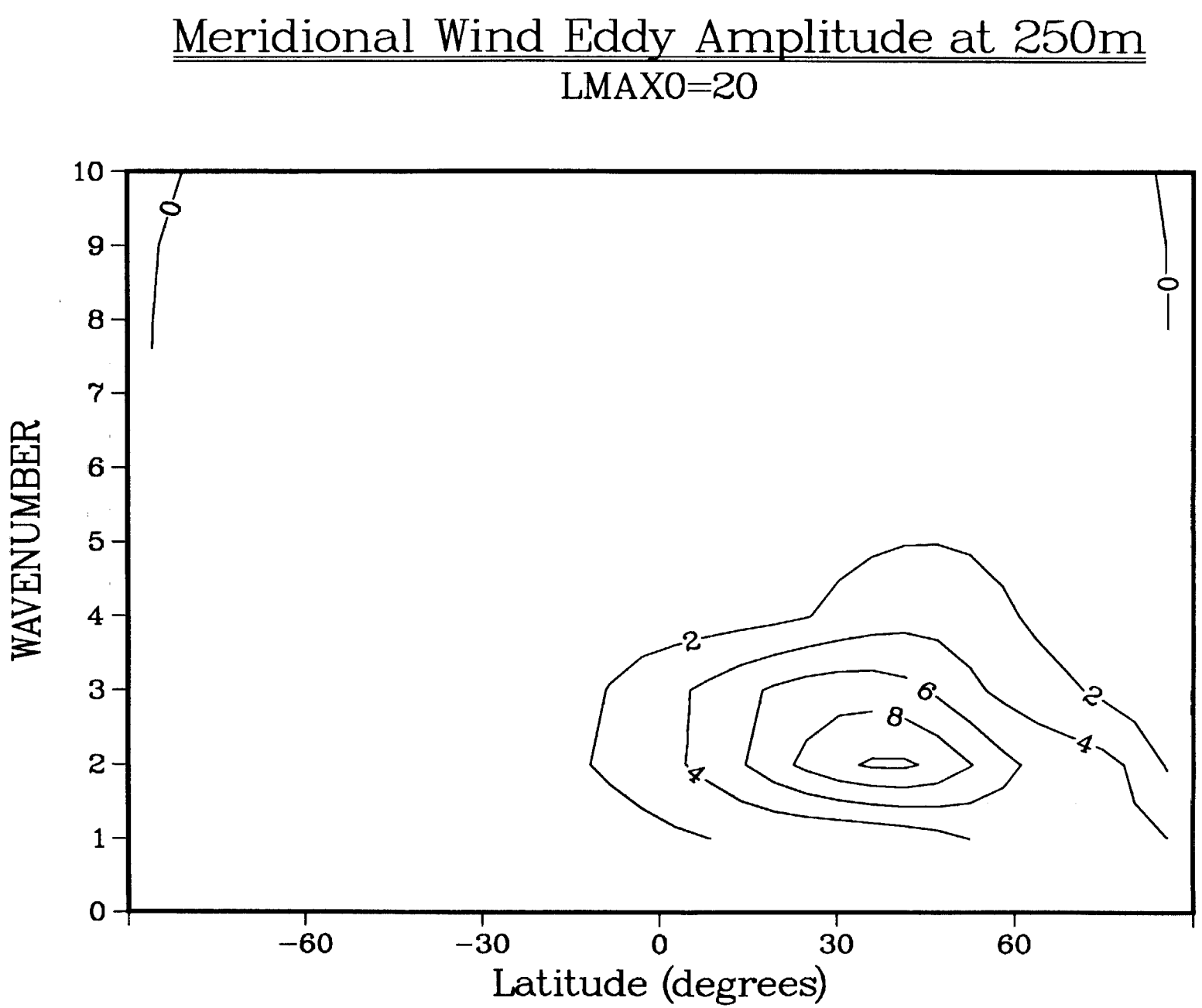
Meridional Wind Eddy Amplitude at 250m
LMAX0=20
WAVENUMBER
10
9
8
7
6
5
4
3
2
1
0
0
0
2
2
4
4
6
8
-60
-30
0
30
60
Latitude (degrees)

Figure 13a.

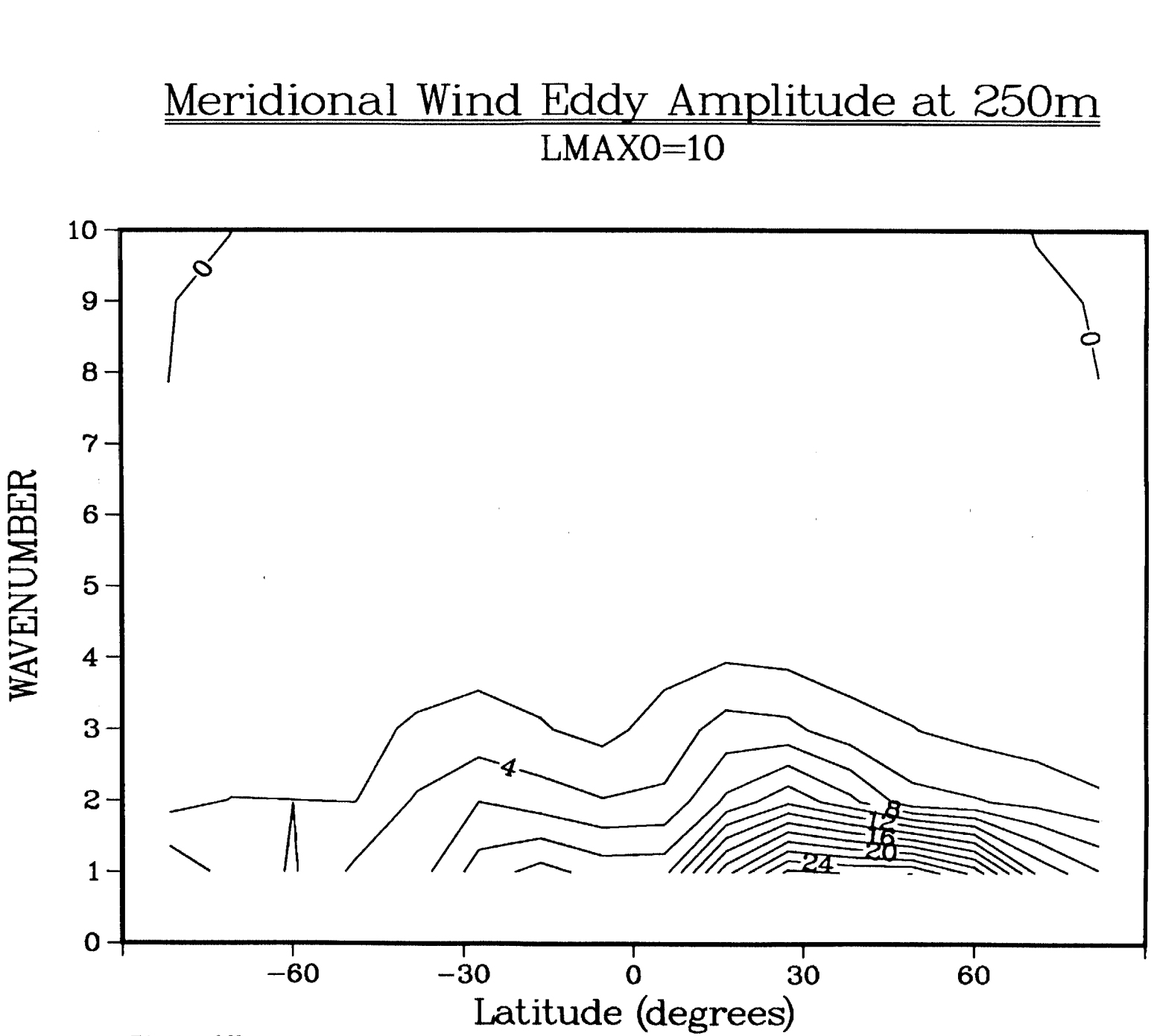
Meridional Wind Eddy Amplitude at 250m
LMAX0=10
WAVENUMBER
10
9
8
7
6
5
4
3
2
1
0
0
0
4
8
12
16
20
24
-60
-30
0
30
60
Latitude (degrees)

Figure 13b.

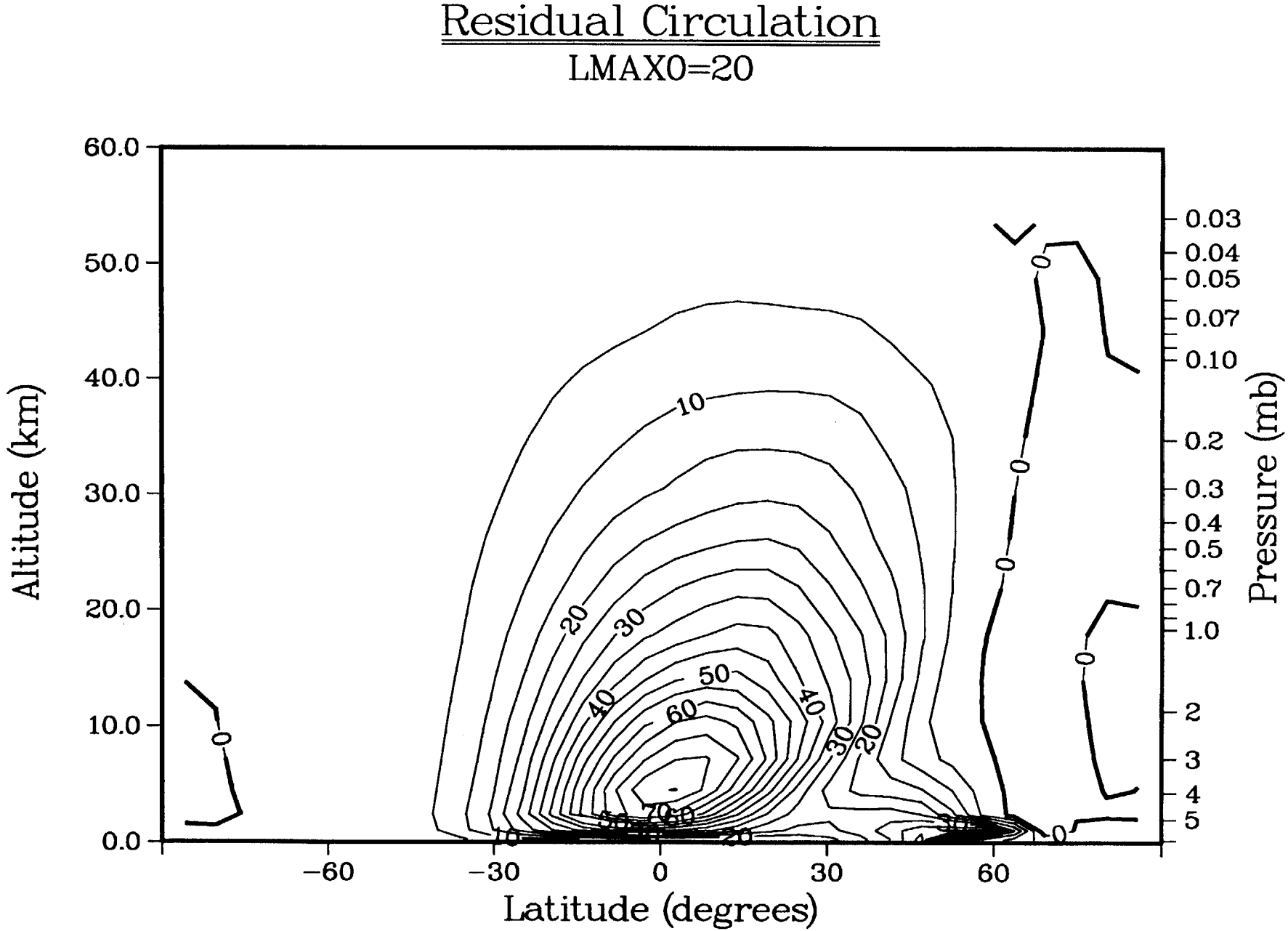
Residual Circulation
LMAX0=20
Altitude (km)
60.0
50.0
40.0
30.0
20.0
10.0
0.0
Pressure (mb)
0.03
0.04
0.05
0.07
0.10
0.2
0.3
0.4
0.5
0.7
1.0
2
3
4
5
−60
−30
0
30
60
Latitude (degrees)
0
10
20
30
40
50
60
70

Figure 14a.

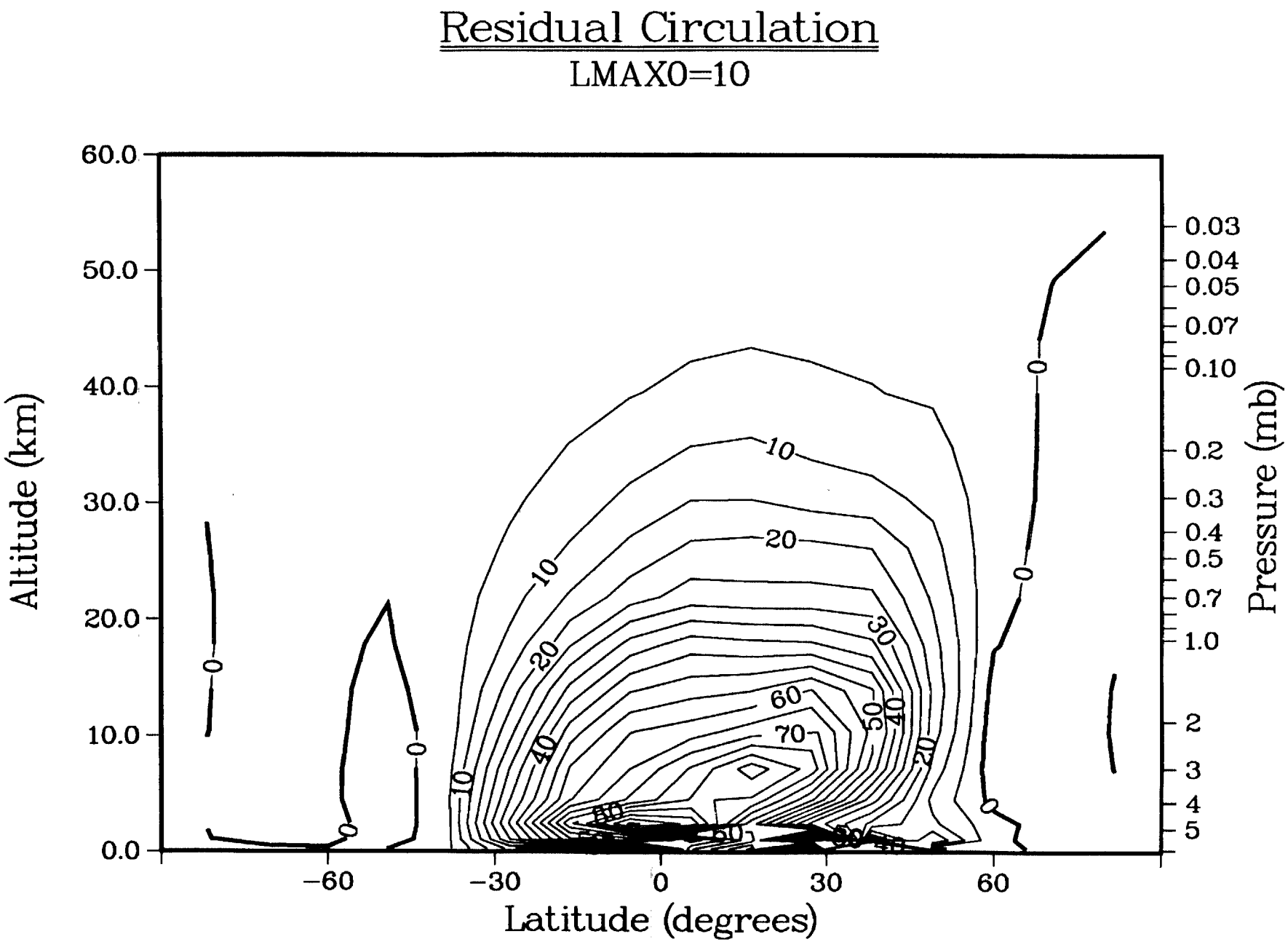
Residual Circulation
LMAX0=10
Altitude (km)
60.0
50.0
40.0
30.0
20.0
10.0
0.0
Pressure (mb)
0.03
0.04
0.05
0.07
0.10
0.2
0.3
0.4
0.5
0.7
1.0
2
3
4
5
-60
-30
0
30
60
Latitude (degrees)
0
10
20
30
40
50
60
70
80

Figure 14b.